

# SPEED: Scalable, Precise, and Efficient Concept Erasure for Diffusion Models

Ouxiang Li<sup>1\*</sup>, Yuan Wang<sup>1\*</sup>, Xinting Hu<sup>2†</sup>, Houcheng Jiang<sup>1</sup>, Tao Liang<sup>3</sup>,  
Yanbin Hao<sup>4</sup>, Guojun Ma<sup>3</sup>, Fuli Feng<sup>1</sup>

<sup>1</sup>University of Science and Technology of China, <sup>2</sup>Nanyang Technological University,

<sup>3</sup>Douyin Co., Ltd., <sup>4</sup>Hefei University of Technology

{lioox, wy1001, jianghc}@mail.ustc.edu.cn, xinting001@e.ntu.edu.sg, taoliangdpg@126.com,  
haoyanbin@hotmail.com, maguojun@bytedance.com, fulifeng93@gmail.com

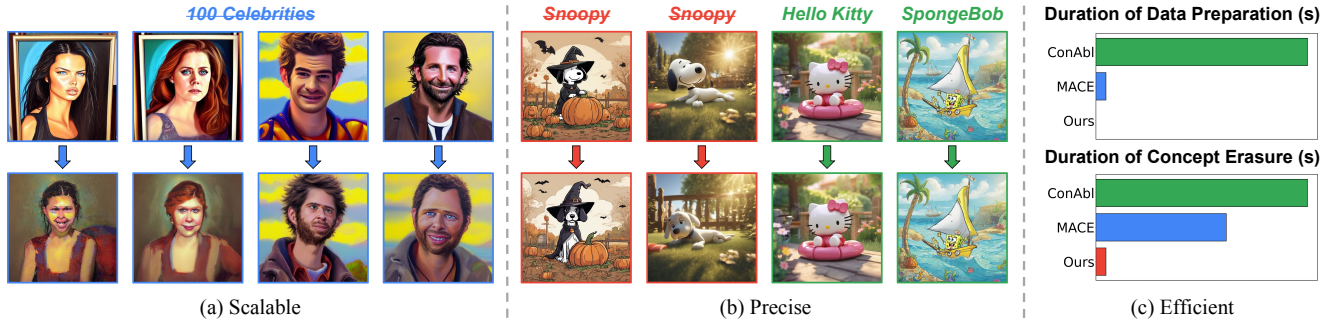


Figure 1. **Three characteristics of our proposed method, SPEED.** (a) **Scalable:** SPEED seamlessly scales from single-concept to large-scale multi-concept erasure (e.g., 100 celebrities) without additional design. (b) **Precise:** SPEED precisely removes the target concept (e.g., *Snoopy*) while preserving the semantic integrity for non-target concepts (e.g., *Hello Kitty* and *SpongeBob*). (c) **Efficient:** SPEED can immediately erase 100 concepts within 5 seconds, achieving a  $\times 350$  speedup over the state-of-the-art (SOTA) method.

## Abstract

Erasing concepts from large-scale text-to-image (T2I) diffusion models has become increasingly crucial due to the growing concerns over copyright infringement, offensive content, and privacy violations. However, existing methods either require costly fine-tuning or degrade image quality for non-target concepts (i.e., prior) due to inherent optimization limitations. In this paper, we introduce *SPEED*, a model editing-based concept erasure approach that leverages null-space constraints for scalable, precise, and efficient erasure. Specifically, *SPEED* incorporates Influence-based Prior Filtering (IPF) to retain the most affected non-target concepts during erasing, Directed Prior Augmentation (DPA) to expand prior coverage while maintaining semantic consistency, and Invariant Equality Constraints (IEC) to regularize model editing by explicitly preserving key invariants during the T2I generation process. Extensive evaluations across multiple concept erasure tasks demonstrate that *SPEED* consistently outperforms existing methods in prior preservation while achieving efficient and high-fidelity concept erasure, successfully removing 100 concepts within just 5 seconds. Our code and models are available at: <https://github.com/Ouxiang-Li/SPEED>.

\*Equal Contributions.

†Corresponding author.

## 1. Introduction

Large-scale text-to-image (T2I) diffusion models [23, 24, 39, 49, 56, 57] have facilitated significant breakthroughs in generating highly realistic and contextually consistent images simply from textual descriptions [7, 11, 13, 16, 44, 46, 50]. Alongside these advancements, concerns have also been raised regarding copyright violations [10, 30, 54], offensive content [51, 65, 67], and privacy concerns [8, 31, 64]. To mitigate ethical and legal risks in generation, it is often necessary to prevent the model from generating certain concepts, a process termed *concept erasure* [17, 29, 66]. However, removing target concepts without carefully preserving the semantics of non-target concepts can introduce unintended artifacts, distortions, and degraded image quality [17, 42, 51, 66], compromising the model’s reliability and usability. Therefore, beyond ensuring the effective removal of target concepts (i.e., *erasure efficacy*), concept erasure should also maintain the original semantics of non-target concepts (i.e., *prior preservation*).

In this context, recent methods seek to balance between erasure efficacy and prior preservation, broadly categorized into two paradigms: training-based [29, 35, 37] and editing-based [18, 19]. The training-based paradigm fine-tunes T2I diffusion models to achieve concept erasure, incorporating an additional regularization term in training for prior preser-

vation. In contrast, the editing-based paradigm is training-free. It jointly optimizes erasure and preservation objectives for target and non-target concepts in a closed-form solution, obtaining direct modifications over model parameters (e.g., projection weights in cross-attention layers [49]). This efficiency also allows editing-based methods to seamlessly extend to multi-concept erasure without additional designs.

However, as the number of target concepts increases, current editing-based methods struggle to balance between erasure efficacy and prior preservation. It can be attributed to the growing conflicts among erasure and preservation objectives, making such trade-offs increasingly difficult. Moreover, these methods rely on weighted least squares optimization [18, 19], inherently imposing a non-zero lower bound on preservation error (Appx. B.2). In multi-concept settings, this accumulation of preservation errors distorts non-target knowledge, further degrading generative quality.

To address the above limitations, we propose **Scalable, Precise, and Efficient Concept Erasure for Diffusion Models (SPEED)** (see Fig. 1), an editing-based method incorporating null-space constraints. Here, we define “null-space” as the subspace that does not alter the feature representations of non-target concepts. By projecting the model parameter updates for erasing concepts onto the null space of non-target concepts, SPEED can minimize the preservation error close to zero without compromising erasure efficacy. A key challenge for SPEED lies in constructing an effective null space based on a set of non-target concepts (i.e., *retain set*). We observe that the existing baseline with null-space constraints [14] confronts a fundamental dilemma during concept erasure: While a narrow retain set limits the prior coverage, increasing the diversity of the retain set restricts the determination of the null space due to rank saturation, thereby compromising prior preservation (see Fig. 2). In this light, we introduce Prior Knowledge Refinement, a suite of techniques that alleviates optimization difficulty and broadens prior coverage.

Particularly, to mitigate optimization difficulty, we propose Influence-based Prior Filtering (IPF), which selectively retains non-target concepts from the retain set that are most affected by the erasure process. These concepts serve as anchors for defining the null space, providing meaningful constraints for preservation while maintaining sufficient flexibility for model editing. To further prevent excessive prior knowledge reduction, we introduce Directed Prior Augmentation (DPA) to enhance prior coverage, which expands the selected retain set after IPF with augmented samples. Instead of simply introducing random noise, we generate semantically consistent variations of preserved concepts, mitigating excessive preservation over meaningless concepts. Furthermore, we incorporate Invariants Equality Constraint (IEC), which identifies critical invariants in the generation process and enforces equality regularization to

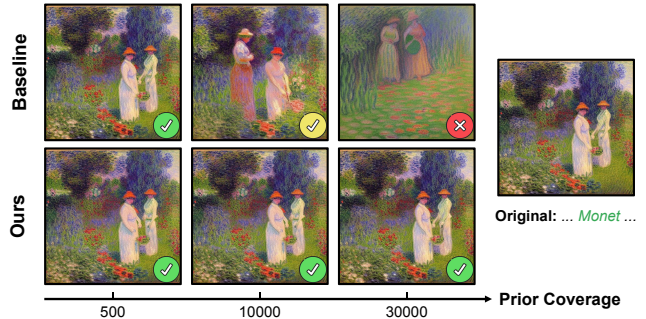


Figure 2. **Impact of the increasing number of non-target concepts in retain set.** The baseline [14] maintains prior preservation with a small retain set (e.g., ✓), but as the retain set grows, rank saturation occurs, leading to gradually degraded semantics in non-target generations (e.g., ⚠ and ✗). In contrast, our method achieves consistent prior preservation by optimizing the retain set.

explicitly preserve them. We evaluate SPEED on three representative concept erasure tasks, i.e., few-concept, multi-concept, and implicit concept erasure, where it consistently exhibits superior prior preservation across all erasure tasks. Overall, our contributions are summarized as follows:

- We propose SPEED, a scalable, precise, and efficient concept erasure method with null-space constrained model editing, capable of erasing 100 concepts in 5 seconds.
- We introduce Prior Knowledge Refinement to construct a well-defined null space that remains meaningful and tractable for editing. By integrating Influence-based Prior Filtering, Directed Prior Augmentation, and Invariants Equality Constraint, it balances rank saturation and prior coverage effectively with precise concept erasure.
- Our extensive experiments show that SPEED consistently outperforms existing methods in prior preservation across various erasure tasks with minimal computational costs.

## 2. Related Works

**Concept erasure.** Current T2I diffusion models inevitably involve unauthorized and NSFW (Not Safe For Work) generations due to the noisy training data from web [52, 53]. Apart from applying additional filters or safety checkers [41, 47, 48], prevailing methods modify diffusion model parameters to erase specific target concepts, mainly categorized into two paradigms. The training-based paradigm fine-tunes model parameters with specific erasure objectives [17, 29, 66] and additional regularization terms [29, 35, 37]. In contrast, the editing-based paradigm edits model parameters using a closed-form solution to facilitate efficiency in concept erasure. For example, UCE [18] modifies model weights by balancing both erasure and preservation error through a weighted least squares objective and RECE [19] iteratively derives new target concept embeddings. These methods can erase numerous concepts within

seconds, demonstrating superior efficiency in practice.

**Null-space constraints.** The null space of a matrix, a fundamental concept in linear algebra, refers to the set of all vectors that the matrix maps to the zero vector. The null-space constraints are first applied to continual learning (CL) by projecting gradients onto the null space of uncentered covariances from previous tasks [60]. Subsequent studies [28, 32, 36, 61, 63] further explore and extend the application of null space in CL. In model editing, AlphaEdit [14] restricts model weight updates onto the null space of preserved knowledge, effectively mitigating trade-offs between editing and preservation. The null-space constraints also apply to various other tasks, *e.g.*, machine unlearning [9] and MRI reconstruction [15], offering great promise for editing-based concept erasure.

### 3. Problem Formulation

#### 3.1. Concept Erasure in Closed-Form Solution

In T2I diffusion models, each concept is encoded by a set of text tokens via CLIP [45], which are then aggregated into a single concept embedding  $\mathbf{c} \in \mathbb{R}^{d_0}$ . For concept erasure, there are two sets of concepts: the erasure set  $\mathbf{E}$  and the retain set  $\mathbf{R}$ . The erasure set consists of  $N_E$  target concepts to be removed, denoted as  $\mathbf{E} = \{\mathbf{c}_1^{(i)}\}_{i=1}^{N_E}$ . The retain set includes  $N_R$  non-target concepts that should be preserved during editing, denoted as  $\mathbf{R} = \{\mathbf{c}_0^{(i)}\}_{i=1}^{N_R}$ . To effectively erase each target concept  $\mathbf{c}_1^{(i)} \in \mathbf{E}$  (*e.g.*, *Snoopy*), it is mapped onto an anchor concept  $\mathbf{c}_*^{(i)}$  that retains general semantics while avoiding the original concept-specific information (*e.g.*, *Dog*). The paired erasure set is denoted as:  $\tilde{\mathbf{E}} = \{(\mathbf{c}_1^{(i)}, \mathbf{c}_*^{(i)})\}_{i=1}^{N_E}$ .

For editing-based methods [18, 19, 42], concept embeddings from the erasure set  $\tilde{\mathbf{E}}$  and the retain set  $\mathbf{R}$  are first organized into three structured matrices:  $\mathbf{C}_1, \mathbf{C}_* \in \mathbb{R}^{d_0 \times N_E}$  and  $\mathbf{C}_0 \in \mathbb{R}^{d_0 \times N_R}$ , which represents the stacked embeddings of the target, anchor, and non-target concepts, respectively. To derive a closed-form solution for concept erasure, existing methods typically optimize a perturbation  $\Delta$  to model parameters  $\mathbf{W}$ , balancing between erasure efficacy and prior preservation. For example, UCE [18] formulates concept erasure as a weighted least squares problem:

$$\Delta_{\text{UCE}} = \arg \min_{\Delta} \underbrace{\|(\mathbf{W} + \Delta)\mathbf{C}_1 - \mathbf{W}\mathbf{C}_*\|_{e_1}^2}_{e_1} + \underbrace{\|\Delta\mathbf{C}_0\|_{e_0}^2}_{e_0}, \quad (1)$$

where the erasure error  $e_1$  ensures that each target concept is mapped onto its corresponding anchor concept and the preservation error  $e_0$  minimizes the impact on non-target priors. This formulation provides a closed-form solution to obtain  $\Delta_{\text{UCE}}$  (see Appx. B.1) for parameter updates, achieving computationally efficient optimization. However, as the number of target concepts increases, the accumu-

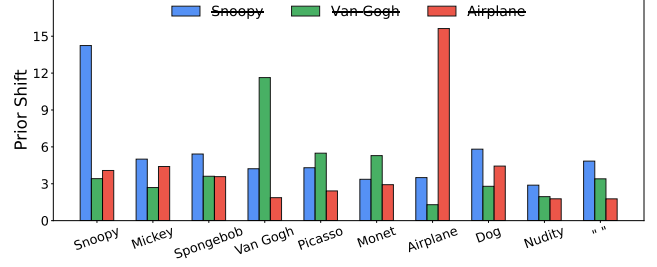


Figure 3. **Prior shift comparison with erasing different target concepts.** The prior shift is measured by  $\|\Delta_{\text{erase}}\mathbf{c}\|^2$  introduced in Sec. 4.1, where  $\mathbf{c}$  denotes the concept embedding. A larger value indicates a greater impact on the concept after erasure.

lated preservation errors  $e_0$  across multiple erased concepts would amplify the distortion on non-target knowledge, further degrading prior preservation.

#### 3.2. Null-Space Constraints

To mitigate the limitation of weighted optimization in prior preservation, SPEED integrates null-space constraints to achieve model editing [14]. These constraints restrict the solution space of  $\Delta$  within the null space of  $\mathbf{C}_0$  to ensure that parameter updates do not interfere with non-target concepts, enforcing  $e_0$  close to zero without a tradeoff between  $e_0$  and  $e_1$ . To obtain  $\Delta$ , we first perform singular value decomposition (SVD) on  $\mathbf{C}_0\mathbf{C}_0^{\top}$  and construct a projection matrix  $\mathbf{P}$ :

$$\{\mathbf{U}, \mathbf{\Lambda}, \mathbf{U}^{\top}\} = \text{SVD}(\mathbf{C}_0\mathbf{C}_0^{\top}), \quad \mathbf{P} = \hat{\mathbf{U}}\hat{\mathbf{U}}^{\top}, \quad (2)$$

where  $\hat{\mathbf{U}}$  is the matrix composed of eigenvectors w.r.t. the zero singular values in  $\mathbf{\Lambda}$ . This projection matrix  $\mathbf{P}$  can map  $\Delta$  onto the null space of  $\mathbf{C}_0$ , *i.e.*,  $\|(\Delta\mathbf{P})\mathbf{C}_0\|^2 = 0$ . Thus, the objective becomes:

$$\begin{aligned} (\Delta\mathbf{P})_{\text{Null}} = \arg \min_{\Delta} & \underbrace{\|(\mathbf{W} + \Delta\mathbf{P})\mathbf{C}_1 - \mathbf{W}\mathbf{C}_*\|_{e_1}^2}_{e_1} \\ & + \underbrace{\|(\Delta\mathbf{P})\mathbf{C}_0\|^2}_{e_0=0} + \underbrace{\|\Delta\mathbf{P}\|^2}_{\text{regularization}}, \end{aligned} \quad (3)$$

where  $\|\Delta\mathbf{P}\|^2$  is an additional regularization term to guarantee convergence. This objective facilitates model parameter editing in the null space of the retain set  $\mathbf{R}$ , showing great promise for prior-preserved concept erasure.

### 4. Prior Knowledge Refinement

The core of null-space constraints in SPEED is to determine a projection matrix  $\mathbf{P}$  that constrains the solution space of  $\Delta$  within the null space of the retain set  $\mathbf{R}$ , ensuring that

\*Considering  $\mathbf{C}_0 \in \mathbb{R}^{d_0 \times N_R}$  may have high dimensionality depending on  $N_R$ , we compute the null space by performing SVD on  $\mathbf{C}_0\mathbf{C}_0^{\top} \in \mathbb{R}^{d_0 \times d_0}$ , as both  $\mathbf{C}_0$  and  $\mathbf{C}_0\mathbf{C}_0^{\top}$  share the same null space.

non-target concepts remain unaffected after erasure. The rank of the matrix  $\mathbf{C}_0\mathbf{C}_0^\top$  reflects the diversity of the retain set, directly shaping the structure of its null space, which is determined by  $\mathbf{R}$ . As  $\mathbf{R}$  increases,  $\mathbf{C}_0\mathbf{C}_0^\top$  gradually reaches full rank, its null space narrows and reduces to the trivial null space  $\{\mathbf{0}\}$ . However, shrinking  $\mathbf{R}$  would eliminate prior coverage by allowing more unintended shifts in non-target concepts not included. To balance this dilemma, we introduce three complementary techniques: Influence-Based Prior Filtering (IPF) to retain the most affected non-target concepts while avoiding excessive rank saturation, Directed Prior Augmentation (DPA) to expand prior coverage with semantically consistent variations, and Invariant Equality Constraints (IEC) to enforce additional constraints to preserve key invariants in generation.

#### 4.1. Influence-Based Prior Filtering (IPF)

Given a pre-defined retain set, existing editing-based methods [18, 19] generally neglect to account for the varying influence of different target concepts on non-target elements, where closer semantic relationships (e.g., *Mickey* and *Dog* for *Snoopy*) lead to greater prior shifts, as shown in Fig. 3. This differing influence suggests that not all non-target concepts contribute equally to preserving prior knowledge, and weakly influenced concepts provide marginal benefit while introducing additional ranks to constrain the null space. To improve, we propose to filter the original retain set by selectively retaining those non-target concepts most influenced by the erased target concepts.

To evaluate this influence, we first obtain the closed-form solution  $\Delta_{\text{erase}}$ , which only considers the erasure efficacy during editing. Specifically, we remove the preservation error  $e_0$  from Eq. 1 and introduce an additional regularization term  $\|\Delta\|^2$  to guarantee convergence:

$$\begin{aligned} \Delta_{\text{erase}} &= \arg \min_{\Delta} \underbrace{\|(\mathbf{W} + \Delta)\mathbf{C}_1 - \mathbf{W}\mathbf{C}_*\|^2}_{e_1} + \underbrace{\|\Delta\|^2}_{\text{regularization}} \\ &= \mathbf{W} (\mathbf{C}_*\mathbf{C}_1^\top - \mathbf{C}_1\mathbf{C}_1^\top) (\mathbf{I} + \mathbf{C}_1\mathbf{C}_1) ^{-1}. \end{aligned} \quad (4)$$

Then we can quantify the influence on each concept embedding  $\mathbf{c}$  by measuring the **prior shift**  $= \|\Delta_{\text{erase}}\mathbf{c}\|^2$ . This metric stems from the intuition that after erasing the target concept, a larger prior shift in the non-target concept indicates a greater influence on the corresponding prior knowledge. Building upon this, we can filter the original retain set  $\mathbf{R}$  with the prior shift by the following process:

$$\mathbf{R}_f : \mathbf{R} \mapsto \{\mathbf{c}_0 \in \mathbf{R} \mid \|\Delta_{\text{erase}}\mathbf{c}_0\|^2 > \mu\}, \quad (5)$$

where the mean value  $\mu = \mathbb{E}_{\mathbf{c}_0 \sim \mathbf{R}} [\|\Delta_{\text{erase}}\mathbf{c}_0\|^2]$  serves as the filtering threshold.

#### 4.2. Directed Prior Augmentation (DPA)

To prevent IPF from generating an overly small retain set, which would compromise prior coverage, an intuitive strat-

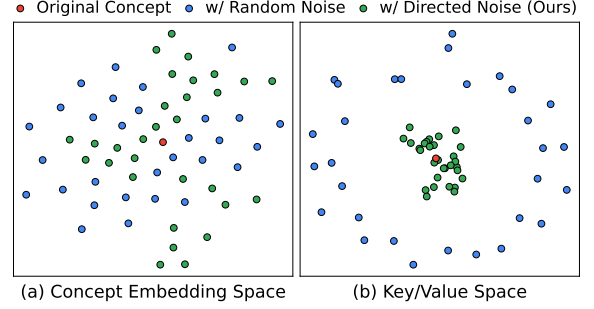


Figure 4. **t-SNE distribution of perturbing the original concept with random noise and our directed noise.** (a) Similar to random noise, our method can span a broad concept embedding space. (b) Our directed noise preserves semantic similarity to the original concept with closer distances in the space mapped by  $\mathbf{W}$ .

egy is to augment the prior knowledge by perturbing the non-target embedding  $\mathbf{c}_0$  with random noise [37]. However, this strategy would introduce meaningless embeddings that fail to generate semantically coherent images (e.g., noise image), resulting in excessive preservation with increasing ranks. To search for more semantically consistent concepts, we introduce directed noise by projecting the random noise  $\epsilon$  onto the direction in which the model parameters  $\mathbf{W}$  exhibit minimal variation. This operation ensures that the perturbed embeddings express closer semantics to the original concept after being mapped by  $\mathbf{W}$ , as shown in Fig. 4. Specifically, we first derive a projection matrix  $\mathbf{P}_{\min}$ :

$$\{\mathbf{U}_{\mathbf{W}}, \Lambda_{\mathbf{W}}, \mathbf{U}_{\mathbf{W}}^\top\} = \text{SVD}(\mathbf{W}), \quad \mathbf{P}_{\min} = \mathbf{U}_{\min}\mathbf{U}_{\min}^\top, \quad (6)$$

where  $\mathbf{U}_{\min} = \mathbf{U}_{\mathbf{W}}[:, -r : ]$  denotes the eigenvectors w.r.t. the smallest  $r$  singular values, which represent the  $r$  least-changing directions of  $\mathbf{W}$ . Then the directed noise  $\epsilon \cdot \mathbf{P}_{\min}$  is used to perturb the original embedding via:

$$\mathbf{c}'_0 = \mathbf{c}_0 + \epsilon \cdot \mathbf{P}_{\min}, \quad \epsilon \sim \mathcal{N}(\mathbf{0}, \mathbf{I}). \quad (7)$$

Given a retain set  $\mathbf{R}$ , the augmentation process can be formulated as follows:

$$\mathbf{R}^{\text{aug}} : \mathbf{R} \mapsto \bigcup_{\mathbf{c}_0 \in \mathbf{R}} \{\mathbf{c}'_{0,k} \mid k = 1, \dots, N_A\}, \quad (8)$$

where  $N_A$  denotes the augmentation times and  $\mathbf{c}'_{0,k}$  represents the  $k$ -th augmented embedding given  $\mathbf{c}_0 \in \mathbf{R}$  using Eq. 7. In implementation, we first filter the original retain set  $\mathbf{R}$  to obtain  $\mathbf{R}_f$  using IPF. Subsequently, further augmentation and filtering are applied to  $\mathbf{R}_f$  using DPA and IPF to obtain  $(\mathbf{R}_f)_f^{\text{aug}}$ , and the two filtered retain sets are then combined together to serve as the final refined retain set  $\mathbf{R}_{\text{refine}} = \mathbf{R}_f \cup (\mathbf{R}_f)_f^{\text{aug}}$ .

#### 4.3. Invariant Equality Constraints (IEC)

In parallel, we also identify certain invariants during the T2I generation process, i.e., intermediate variables that remain

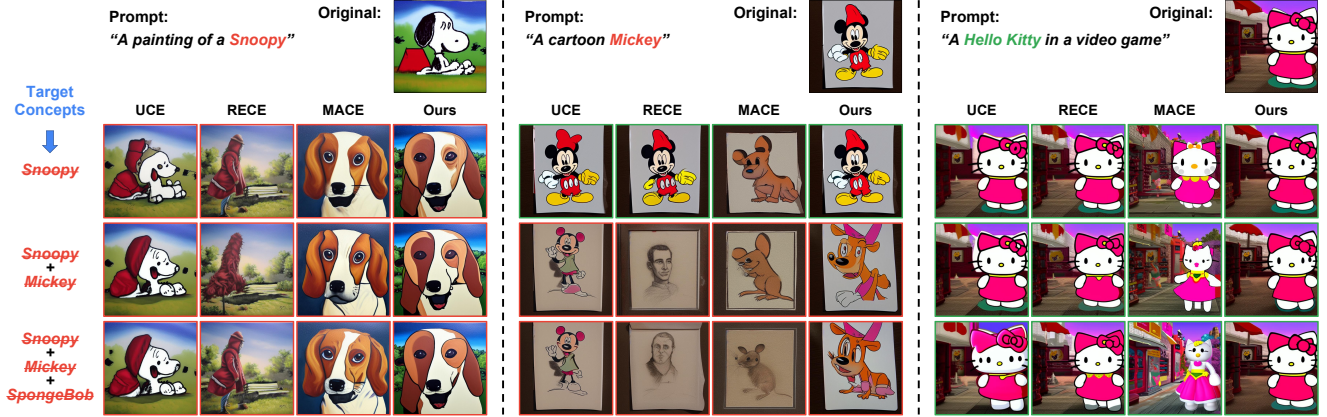


Figure 5. **Qualitative comparison of the few-concept erasure in erasing single and multiple instances.** The erased and preserved generations are highlighted with **red** and **green** boxes, respectively. Our method demonstrates superior prior preservation compared to the SOTA method, UCE [18], in single-concept erasure, and this superiority is amplified as the target concepts increase. For example, in the *Hello Kitty* case, our generation exhibits less alteration after erasing three concepts, whereas UCE’s generations are gradually deteriorating.

unchanged with sampling prompts. One such invariant is the CLIP-encoded  $[SOT]$  token. Since the encoding process is masked by causal attention and all prompts are prefixed with the fixed  $[SOT]$  token during tokenization, the corresponding embedding remains unchanged. Another invariant is the null-text embedding, as it corresponds to the unconditional generation under the classifier-free guidance [23], which also remains unchanged despite prompt variations. Given the invariance of these embeddings, we consider additional protection measures for these invariant embeddings to ensure their outputs remain unchanged during concept erasure. Specifically, we introduce explicit equality constraints for invariants based on Eq. 3:

$$\min_{\Delta} \underbrace{\|(\mathbf{W} + \Delta\mathbf{P})\mathbf{C}_1 - \mathbf{W}\mathbf{C}_*\|^2}_{e_1} + \underbrace{\|\Delta\mathbf{P}\|^2}_{\text{regularization}}, \quad (9)$$

$$\text{s.t. } \underbrace{(\Delta\mathbf{P})\mathbf{C}_2 = \mathbf{0}}_{\text{equality constraints}}$$

where  $\mathbf{C}_2$  denotes the stacked invariant embedding matrix of  $[SOT]$  and null-text<sup>†</sup>. With the projection matrix  $\mathbf{P}$  derived from  $\mathbf{R}_{\text{refine}}$ , we can compute the closed-form solution of Eq. 9 using Lagrange Multipliers from Appx. B.3:

$$(\Delta\mathbf{P})_{\text{SPEED}} = \mathbf{W} (\mathbf{C}_*\mathbf{C}_1^\top - \mathbf{C}_1\mathbf{C}_1^\top) \mathbf{P}\mathbf{Q}\mathbf{M}, \quad (10)$$

where

$$\mathbf{M} = (\mathbf{C}_1\mathbf{C}_1^\top\mathbf{P} + \mathbf{I})^{-1}, \quad (11)$$

$$\mathbf{Q} = \mathbf{I} - \mathbf{M}\mathbf{C}_2 (\mathbf{C}_2^\top\mathbf{P}\mathbf{M}\mathbf{C}_2)^{-1} \mathbf{C}_2^\top\mathbf{P}.$$

This closed-form solution enforces the equality constraints by projecting the parameter update onto the subspace or-

<sup>†</sup>Since the null-text embeddings are only composed of  $[EOT]$  tokens (excluding  $[SOT]$ ), we use the k-means algorithm [38] to select k centroids to reduce redundancy.

thogonal to the invariant embeddings. Since image generation inevitably depends on these invariant embeddings, such constraints inherently preserve prior knowledge.

## 5. Experiments

In this section, we conduct extensive experiments on three representative erasure tasks, including few-concept erasure, multi-concept erasure, and implicit concept erasure, validating our superior prior preservation. The compared baselines include ConAbl [29], MACE [35], RECE [19], and UCE [18], which have achieved SOTA performance across various concept erasure tasks. In implementation, we conduct all experiments on SDv1.4 [1] and generate each image using DPM-solver sampler [34] over 20 sampling steps with classifier-free guidance [23] of 7.5. More implementation details and compared baselines (e.g., SPM [37]) can be found in Appx. C and Appx. D.2.

### 5.1. On Few-Concept Erasure

**Evaluation setup.** To compare the few-concept erasure performance with baseline methods, we conduct experiments on instance erasure and artistic style erasure following [37], where all methods are evaluated based on 80 instance templates and 30 artistic style templates, generating 10 images per template per concept. We use two metrics for evaluation: CLIP Score (CS) [45] measuring the text-image similarity and Fréchet Inception Distance (FID) [22] assessing the distributional distance before and after erasure. Following [37], we select non-target concepts with similar semantics to the target concept for comparison and report CS for targets and FID for non-targets in the main paper. Full comparisons are presented in Appx. D.1. We further compare the generations on MS-COCO captions [33], where we generate images with the first 1,000 captions, and report the CS

| Concept                                                    | <i>Snoopy</i> | <i>Mickey</i> | <i>Spongebob</i> | <i>Pikachu</i> | <i>Hello Kitty</i> | MS-COCO      |              |
|------------------------------------------------------------|---------------|---------------|------------------|----------------|--------------------|--------------|--------------|
|                                                            | CS            | CS            | CS               | CS             | CS                 | CS           | FID          |
| SD v1.4                                                    | 28.51         | 26.62         | 27.30            | 27.44          | 27.77              | 26.53        | -            |
| Erase <i>Snoopy</i>                                        |               |               |                  |                |                    |              |              |
|                                                            | CS ↓          | FID ↓         | FID ↓            | FID ↓          | FID ↓              | CS ↑         | FID ↓        |
| ConAbl                                                     | 25.44         | 37.08         | 38.92            | 26.14          | 36.52              | 26.40        | 21.20        |
| MACE                                                       | 20.90         | 105.97        | 102.77           | 65.71          | 75.42              | 26.09        | 42.62        |
| RECE                                                       | <b>18.38</b>  | 26.63         | 34.42            | 21.99          | 32.35              | 26.39        | 25.61        |
| UCE                                                        | 23.19         | 24.87         | 29.86            | 19.06          | 27.86              | 26.46        | 22.18        |
| Ours                                                       | 23.50         | <b>23.41</b>  | <b>24.64</b>     | <b>16.81</b>   | <b>21.74</b>       | <b>26.48</b> | <b>19.95</b> |
| Erase <i>Snoopy</i> and <i>Mickey</i>                      |               |               |                  |                |                    |              |              |
|                                                            | CS ↓          | CS ↓          | FID ↓            | FID ↓          | FID ↓              | CS ↑         | FID ↓        |
| ConAbl                                                     | 25.26         | 26.58         | 45.08            | 35.57          | 41.48              | 26.42        | 24.34        |
| MACE                                                       | 20.53         | 20.63         | 112.01           | 91.72          | 106.88             | 25.50        | 55.15        |
| RECE                                                       | <b>18.57</b>  | <b>18.14</b>  | 35.85            | 26.05          | 40.77              | 26.31        | 30.30        |
| UCE                                                        | 23.60         | 24.79         | 30.58            | 23.51          | 31.76              | 26.38        | 26.06        |
| Ours                                                       | 23.58         | 23.62         | <b>29.67</b>     | <b>22.51</b>   | <b>28.23</b>       | <b>26.47</b> | <b>23.66</b> |
| Erase <i>Snoopy</i> and <i>Mickey</i> and <i>Spongebob</i> |               |               |                  |                |                    |              |              |
|                                                            | CS ↓          | CS ↓          | CS ↓             | FID ↓          | FID ↓              | CS ↑         | FID ↓        |
| ConAbl                                                     | 24.92         | 26.46         | 25.12            | 46.47          | 48.24              | 26.37        | 26.71        |
| MACE                                                       | 19.86         | 19.35         | 20.12            | 110.12         | 128.56             | 23.39        | 66.39        |
| RECE                                                       | <b>18.17</b>  | <b>18.87</b>  | <b>16.23</b>     | 40.52          | 52.06              | 26.32        | 32.51        |
| UCE                                                        | 23.29         | 24.63         | 19.08            | 29.20          | 38.15              | 26.30        | 28.71        |
| Ours                                                       | 23.69         | 23.93         | 21.39            | <b>21.40</b>   | <b>26.22</b>       | <b>26.51</b> | <b>24.99</b> |

Table 1. **Quantitative comparison of the few-concept erasure in erasing instances**, where the erased target concept(s) are shaded in pink. Arrows on the headers indicate the preferred direction for each metric, and the best results are highlighted in bold. Our method, which does not achieve the lowest CS but has been proven sufficient in Fig. 5, consistently demonstrates significant improvements in prior preservation for non-target concepts.

and FID as the measure of general knowledge preservation. **Analysis and discussion.** Tables 1 and 2 compare the results of erasing various instance concepts and artistic styles. Our method consistently achieves the lowest FIDs across all non-target concepts, demonstrating superior prior preservation with minimal alteration to the original content. Moreover, we emphasize that our erasure is sufficiently effective, even without achieving the lowest CS, as shown in Fig. 5. In contrast, lower CS values typically indicate over-erasure, which results in excessive degradation of prior knowledge. Notably, with the number of target concepts increasing from 1 to 3, our FID in *Pikachu* rises from 16.81 to 21.40 (4.59 ↑), while UCE increases from 19.06 to 29.20 (10.14 ↑). A similar pattern is observed in *Hello Kitty* (Our 4.48 ↑ v.s. UCE’s 10.29 ↑), showing the robustness of our method in erasing increasing multiple concepts.

## 5.2. On Multi-Concept Erasure

**Evaluation setup.** Another more realistic erasure scenario is multi-concept erasure, where massive concepts are required to be erased at once. Herein, we follow the experiment setup in [35] for erasing multiple celebrities, where we experiment with erasing 10, 50, and 100 celebrities and collect another 100 celebrities as non-target concepts. We

| Concept               | <i>Van Gogh</i> | <i>Picasso</i> | <i>Monet</i> | <i>Paul Gauguin</i> | <i>Caravaggio</i> | MS-COCO      |              |
|-----------------------|-----------------|----------------|--------------|---------------------|-------------------|--------------|--------------|
|                       | CS              | CS             | CS           | CS                  | CS                | CS           | FID          |
| SD v1.4               | 28.75           | 27.98          | 28.91        | 29.80               | 26.27             | 26.53        | -            |
| Erase <i>Van Gogh</i> |                 |                |              |                     |                   |              |              |
|                       | CS ↓            | FID ↓          | FID ↓        | FID ↓               | FID ↓             | CS ↑         | FID ↓        |
| ConAbl                | 28.16           | 77.01          | 63.80        | 63.20               | 79.25             | 26.46        | <b>18.36</b> |
| MACE                  | 26.66           | 69.92          | 60.88        | 56.18               | 69.04             | 26.50        | 23.15        |
| RECE                  | 26.39           | 60.57          | 61.09        | 47.07               | 72.85             | 26.52        | 23.54        |
| UCE                   | 28.10           | 43.02          | 40.49        | 32.62               | 61.72             | 26.54        | 19.63        |
| Ours                  | <b>26.29</b>    | <b>35.86</b>   | <b>16.85</b> | <b>24.94</b>        | <b>39.75</b>      | <b>26.55</b> | 20.36        |
| Erase <i>Picasso</i>  |                 |                |              |                     |                   |              |              |
|                       | FID ↓           | CS ↓           | FID ↓        | FID ↓               | FID ↓             | CS ↑         | FID ↓        |
| ConAbl                | 60.44           | 26.97          | 36.23        | 65.23               | 79.12             | 26.43        | 20.02        |
| MACE                  | 59.58           | 26.48          | 37.02        | 46.35               | 66.20             | 26.47        | 22.86        |
| RECE                  | 51.09           | 26.66          | 25.39        | 46.08               | 75.61             | 26.48        | 23.03        |
| UCE                   | 37.58           | 26.99          | <b>16.72</b> | 32.48               | 59.27             | 26.50        | 20.33        |
| Ours                  | <b>19.18</b>    | <b>26.22</b>   | 19.87        | <b>24.73</b>        | <b>43.63</b>      | <b>26.51</b> | <b>19.98</b> |
| Erase <i>Monet</i>    |                 |                |              |                     |                   |              |              |
|                       | FID ↓           | FID ↓          | CS ↓         | FID ↓               | FID ↓             | CS ↑         | FID ↓        |
| ConAbl                | 68.77           | 64.25          | 27.05        | 57.33               | 71.88             | 26.45        | 21.03        |
| MACE                  | 61.50           | 48.41          | 25.98        | 49.66               | 65.87             | 26.47        | 22.76        |
| RECE                  | 56.26           | 45.97          | 25.87        | 46.38               | 64.19             | 26.49        | 24.94        |
| UCE                   | 42.25           | <b>38.73</b>   | 27.12        | 33.00               | 56.49             | <b>26.51</b> | 21.58        |
| Ours                  | <b>28.78</b>    | 41.21          | <b>25.06</b> | <b>27.85</b>        | <b>55.20</b>      | 26.48        | <b>20.87</b> |

Table 2. **Quantitative comparison of the few-concept erasure in erasing single artistic style.**

prepare 5 prompt templates for each celebrity concept. For non-target concepts, we generate 1 image per template for each of the 100 concepts, totaling 500 images. For target concepts, we adjust the per-concept quantity to maintain a total of 500 images (e.g., erasing 10 celebrities involves generating 10 images with 5 templates per concept). In evaluation, we adopt GIPHY Celebrity Detector (GCD) [20] and measure the top-1 GCD accuracy, indicated by  $Acc_e$  for erased target concepts and  $Acc_r$  for retained non-target concepts. Meanwhile, the harmonic mean  $H_o$  is adopted to assess the overall erasure performance:

$$H_o = \frac{2}{(1 - Acc_e)^{-1} + (Acc_r)^{-1}}. \quad (12)$$

Additionally, we report the results on MS-COCO to demonstrate the prior preservation of general concepts.

**Analysis and discussion.** Table 3 showcases a notable improvement of our method on multi-concept erasure, particularly in prior preservation with the highest  $Acc_r$ . In comparison with the SOTA method, MACE [35], our method achieves superior prior preservation with better  $Acc_r$ , while maintaining comparable erasure efficacy, as reflected in similar  $Acc_e$ , resulting in the best overall erasure performance indicated by the highest  $H_o$ . Meanwhile, our method attains the lowest FID across all methods on MS-COCO. The other methods, UCE [18] and RECE [19], although achieving considerable balance in few-concept erasure, fail to maintain this balance as the number of target concepts increases as shown in Fig. 6, with catastrophic prior dam-

|         | Erase 10 Celebrities |                    |                  | MS-COCO      |              | Erase 50 Celebrities |                    |                  | MS-COCO      |              | Erase 100 Celebrities |                    |                  | MS-COCO      |              |
|---------|----------------------|--------------------|------------------|--------------|--------------|----------------------|--------------------|------------------|--------------|--------------|-----------------------|--------------------|------------------|--------------|--------------|
|         | Acc <sub>e</sub> ↓   | Acc <sub>r</sub> ↑ | H <sub>o</sub> ↑ | CS ↑         | FID ↓        | Acc <sub>e</sub> ↓   | Acc <sub>r</sub> ↑ | H <sub>o</sub> ↑ | CS ↑         | FID ↓        | Acc <sub>e</sub> ↓    | Acc <sub>r</sub> ↑ | H <sub>o</sub> ↑ | CS ↑         | FID ↓        |
| SD v1.4 | 91.99                | 89.66              | 14.70            | 26.53        | -            | 93.08                | 89.66              | 12.85            | 26.53        | -            | 90.18                 | 89.66              | 17.70            | 26.53        | -            |
| UCE     | 0.20                 | 71.19              | 83.10            | 24.07        | 83.81        | 0.00                 | 31.94              | 48.41            | 13.45        | 209.93       | 0.00                  | 20.92              | 34.60            | 13.49        | 185.46       |
| RECE    | 0.34                 | 67.43              | 80.44            | 16.75        | 170.65       | 1.03                 | 19.77              | 32.95            | 13.49        | 213.39       | 2.43                  | 23.71              | 38.16            | 12.09        | 177.57       |
| MACE    | 1.62                 | 87.73              | 92.75            | 26.36        | 37.25        | 3.41                 | 84.31              | 90.03            | 25.45        | 45.31        | 4.80                  | 80.20              | 87.06            | 24.80        | 50.41        |
| Ours    | 1.81                 | 89.09              | <b>93.42</b>     | <b>26.47</b> | <b>30.02</b> | 3.46                 | 88.48              | <b>92.34</b>     | <b>26.46</b> | <b>39.23</b> | 5.87                  | 85.54              | <b>89.63</b>     | <b>26.22</b> | <b>44.97</b> |

Table 3. **Quantitative comparison of the multi-concept erasure in erasing 10, 50, and 100 celebrities.** The best results are highlighted in **bold**. Our method is capable of erasing up to 100 celebrities at once with low Acc<sub>e</sub> (%) and preserving other non-target celebrities with less appearance alteration with high Acc<sub>r</sub> (%), resulting in the best overall erasure performance H<sub>o</sub> (shaded in pink).

|         | NudeNet Detection Results on I2P |       |          |      |             |               |             |               |            |              | MS-COCO      |  |
|---------|----------------------------------|-------|----------|------|-------------|---------------|-------------|---------------|------------|--------------|--------------|--|
|         | Armpits                          | Belly | Buttocks | Feet | Breasts (F) | Genitalia (F) | Breasts (M) | Genitalia (M) | Total ↓    | CS ↑         | FID ↓        |  |
| SD v1.4 | 123                              | 134   | 19       | 14   | 258         | 9             | 16          | 3             | 576        | 26.53        | -            |  |
| ConAbl  | 24                               | 43    | 5        | 6    | 68          | 1             | 6           | 4             | 157        | 26.14        | 39.26        |  |
| MACE    | 28                               | 19    | 1        | 20   | 37          | 3             | 6           | 5             | 119        | 24.06        | 52.78        |  |
| RECE    | 17                               | 29    | 3        | 7    | 14          | 1             | 8           | 1             | <b>80</b>  | 25.98        | 40.37        |  |
| UCE     | 29                               | 42    | 2        | 11   | 36          | 3             | 9           | 7             | 139        | <u>26.24</u> | <u>38.60</u> |  |
| Ours    | 20                               | 42    | 7        | 3    | 29          | 2             | 5           | 5             | <u>113</u> | <b>26.29</b> | <b>37.82</b> |  |

Table 4. **Evaluation of implicit concept erasure on I2P benchmark.** We report the number of nude body parts (F: Female, M: Male) detected by the NudeNet with threshold = 0.6. The best and second-best results are marked in **bold** and underlined. (Left) Our method effectively removes nude content, even though *nudity* is not explicitly mentioned in prompts from I2P, achieving the second-best total count. (Right) Our method also consistently achieves superior prior preservation for non-target concepts to other methods on MS-COCO.

age evidenced by MS-COCO as well. Notably, our method can erase up to 100 celebrities in 5 seconds, whereas MACE requires around 30 minutes (×350 time). In real-world scenarios, this efficiency underscores our potential for the instant erasure of massive concepts.

### 5.3. On Implicit Concept Erasure

**Evaluation setup.** We further evaluate the erasure efficacy on implicit concepts, where the target concept does not explicitly appear in the text prompt. We conduct experiments on the Inappropriate Image Prompt (I2P) benchmark [51], which consists of various implicit inappropriate prompts involving violence, sexual content, and nudity. We follow the same setting in [19] to erase *nudity* → ‘ ’. Specifically, we generate images using all 4,703 text prompts in I2P and use NudeNet [6] to identify if the nude content is successfully erased with the threshold of 0.6. Additionally, we report the results on MS-COCO to demonstrate the prior preservation of general concepts.

**Analysis and discussion.** As shown in Table 4, our method can effectively erase the implicit concept, *i.e.*, *nudity*, with the second-best number of detected nude body parts. The SOTA method, RECE [19], achieves the best total number by extending the erasure set with more target concepts, but this comes at the cost of sacrificing prior preservation on MS-COCO. In contrast, our method achieves the best prior preservation, demonstrating effective erasure while main-

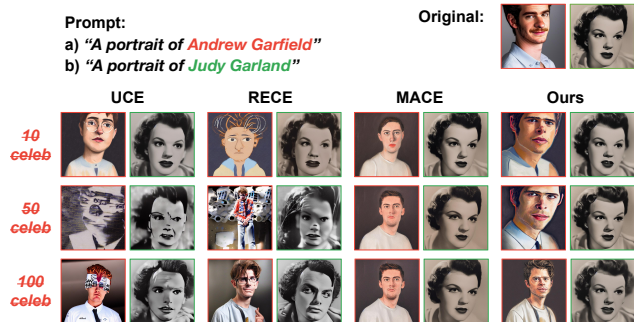


Figure 6. **Quantitative comparison of multi-concept erasure** in erasing different numbers of celebrities (celeb). The erased and preserved generations are highlighted with **red** and **green** boxes, respectively. Our method can precisely erase 100 celebrities while maintaining the proper generation of other non-target concepts.

taining strong prior preservation, striking a favorable balance between erasure and preservation.

### 5.4. Further Analysis

**Duration comparison.** Table 5 presents the duration comparison in erasing 1, 10, and 100 concepts across different methods. It is obvious that training-based methods necessitate significantly higher computational costs than editing-based ones. In contrast, our method achieves precise multi-concept erasure in a remarkably short time, demonstrating superior efficiency while maintaining erasure performance,

|                     | Training-based     |                          | Editing-based |      |      |
|---------------------|--------------------|--------------------------|---------------|------|------|
|                     | ConAbl             | MACE                     | UCE           | RECE | Ours |
| <b>Data Prepare</b> | $n \times 1000t_1$ | $n \times (8t_1 + 8t_2)$ | 0             | 0    | 0    |
| <b>1-concept</b>    | $1 \times 90$      | 55.1                     | 1.2           | 1.5  | 3.6  |
| <b>10-concepts</b>  | $10 \times 90$     | 207.0                    | 1.5           | 2.5  | 3.8  |
| <b>100-concepts</b> | $100 \times 90$    | 1750.9                   | 2.1           | 11.0 | 5.0  |

Table 5. **Duration comparison (s) in erasing multiple celebrities** on one A100 GPU, where  $n$  is the number of target concepts. During data preparation, ConAbl requires pre-sampling 1,000 images ( $t_1$  per image) for each target concept while MACE needs 8 pre-sampled images along with 8 corresponding segmentation masks ( $t_2$  per mask) using SAM [27].

| Ablation | Components |     |     |     | Target       | Non-Target   | MS-COCO      |              |
|----------|------------|-----|-----|-----|--------------|--------------|--------------|--------------|
|          | IEC        | IPF | RPA | DPA | CS ↓         | FID ↓        | CS ↑         | FID ↓        |
| 1        | ×          | ×   | ×   | ×   | 27.20        | 50.43        | 26.42        | 26.33        |
| 2        | ✓          | ×   | ×   | ×   | 27.20        | 48.17        | 26.44        | 24.95        |
| 3        | ✓          | ✓   | ×   | ×   | 26.68        | 38.02        | 26.54        | 20.57        |
| 4        | ✓          | ✓   | ✓   | ×   | 26.30        | 32.62        | 26.52        | 20.99        |
| Ours     | ✓          | ✓   | ×   | ✓   | <b>26.29</b> | <b>29.35</b> | <b>26.55</b> | <b>20.36</b> |
| SD v1.4  | -          | -   | -   | -   | 28.75        | -            | 26.53        | -            |

Table 6. **Ablation study on the proposed components** in erasing *Van Gogh*, with the non-target FID averaged over other four styles (i.e., *Picasso*, *Monet*, *Paul Gauguin*, *Caravaggio*) as in Table 2. Ablation 1 corresponds to the original objective from [14] in Eq. 3. The ablated components include: IEC (Invariant Equality Constraints), IPF (Influence-based Prior Filtering), RPA (Random Prior Augmentation), and DPA (Directed Prior Augmentation).

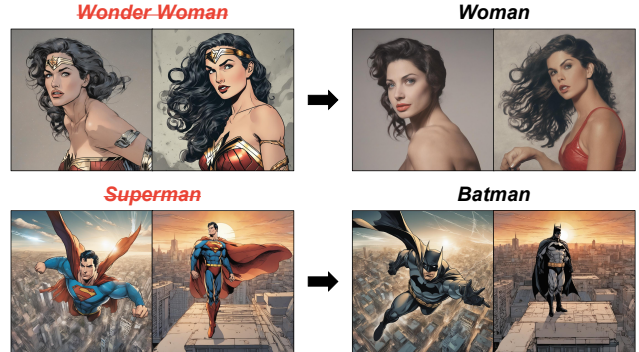
as evidenced in Table 3.

**Component ablation.** In Table 6, we compare the individual impact of our components on prior preservation and draw the following conclusions: (1) Impact of IEC (Ablation 1 v.s. 2): IEC reduces the non-target FID and the MS-COCO FID, demonstrating its effectiveness by preserving invariant embeddings with equality constraints. (2) Impact of IPF (Ablation 2 v.s. 3): Incorporating IPF results in a significant improvement in both FIDs, underscoring its critical role in filtering out less-influenced concepts in the retain set under rank saturation. (3) Impact of DPA (Ablation 4 v.s. Ours): DPA improves RPA with directed noise and leads to a substantial improvement in non-target and MS-COCO FIDs, highlighting its advantage by introducing semantically similar concepts into the refined retain set. To conclude, the proposed three components (i.e., IEC, IPF, and DPA) improve the prior preservation from different perspectives and contribute to our method with the best prior preservation under null space constraints.

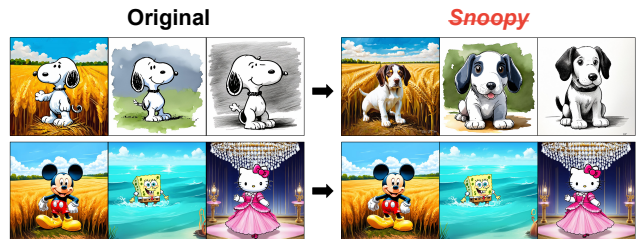
**More applications on other T2I models.** To validate the transferability of our method across versatile applications, we conduct further experiments on various T2I models with different weights and architectures, including: (1) Composite concept erasure on DreamShaper [3] and RealisticVi-



(a) Composite Concept Erasure on Community Versions



(b) Knowledge Editing on SDXL



(c) Instance Erasure and Prior Preservation on SDv3

Figure 7. **More applications across various T2I diffusion models.** (a) We conduct both single and composite concept erasure for “*Snoopy + Van Gogh*” on two community T2I models [3, 4]. (b) Our method also enables model knowledge editing by specifying the anchor concept, such as “*Wonder Woman* → *Woman*” and “*Superman* → *Batman*” on SDXL [44]. (c) Our method can seamlessly transfer to novel DiT-based T2I models (e.g., SDv3 [13]).

sion [4] from Fig 7 (a): Our method can precisely erase the target concept(s) while preserving other non-target elements within the prompt, such as the *Van Gogh*-style background (2nd column) and the *Snoopy* character (3rd column). (2) Knowledge editing on SDXL [44] from Fig 7 (b): The arbitrary nature of anchor concepts allows us to edit the pre-trained model knowledge while maintaining the overall layout and semantics of the generated images. Herein, our method effectively edits the model knowledge while maintaining the overall layout and semantics of the generated images. (3) Instance erasure on SDv3 [13] from Fig 7 (c): To accommodate the diffusion transformer (DiT) [43] architecture in T2I models, we adapt our method to a DiT-based model, demonstrating a well-balanced trade-off between erasure (1st row) and preservation (2nd row) as well.

## 6. Conclusion

This paper introduced SPEED, a scalable, precise, and efficient concept erasure method for T2I diffusion models. It formulates concept erasure as a null-space constrained optimization problem, facilitating effective prior preservation along with precise erasure efficacy. Critically, SPEED overcomes the inefficacy of editing-based methods in multi-concept erasure while circumventing the prohibitive computational costs associated with training-based approaches. With our proposed Prior Knowledge Refinement involving three complementary techniques, SPEED not only ensures superior prior preservation but also achieves a  $350\times$  acceleration in multi-concept erasure, establishing itself as a scalable and practical solution for real-world applications.

## References

- [1] Stable diffusion. <https://huggingface.co/CompVis/stable-diffusion-v1-4>, 2022. 5, 15, 18
- [2] Stable diffusion v2.1. <https://huggingface.co/stabilityai/stable-diffusion-2-1>, 2022. 18
- [3] Dreamshaper. <https://huggingface.co/Lykon/dreamshaper-8>, 2023. 8
- [4] Realisticvision. [https://huggingface.co/SG161222/Realistic\\_Vision\\_V5.1\\_noVAE](https://huggingface.co/SG161222/Realistic_Vision_V5.1_noVAE), 2023. 8
- [5] Josh Achiam, Steven Adler, Sandhini Agarwal, Lama Ahmad, Ilge Akkaya, Florencia Leoni Aleman, Diogo Almeida, Janko Altschmidt, Sam Altman, Shyamal Anadkat, et al. Gpt-4 technical report. *arXiv preprint arXiv:2303.08774*, 2023. 15
- [6] P Bedapudi. Nudenet: Neural nets for nudity classification, detection and selective censoring, 2019. 7, 15
- [7] James Betker, Gabriel Goh, Li Jing, Tim Brooks, Jianfeng Wang, Linjie Li, Long Ouyang, Juntang Zhuang, Joyce Lee, Yufei Guo, et al. Improving image generation with better captions. *Computer Science*. <https://cdn.openai.com/papers/dall-e-3.pdf>, 2(3):8, 2023. 1
- [8] Nicolas Carlini, Jamie Hayes, Milad Nasr, Matthew Jagielski, Vikash Sehwal, Florian Tramèr, Borja Balle, Daphne Ippolito, and Eric Wallace. Extracting training data from diffusion models. In *32nd USENIX Security Symposium (USENIX Security 23)*, pages 5253–5270, 2023. 1
- [9] Huiqiang Chen, Tianqing Zhu, Xin Yu, and Wanlei Zhou. Machine unlearning via null space calibration. *arXiv preprint arXiv:2404.13588*, 2024. 3
- [10] Yingqian Cui, Jie Ren, Han Xu, Pengfei He, Hui Liu, Lichao Sun, Yue Xing, and Jiliang Tang. Diffusionshield: A watermark for copyright protection against generative diffusion models. *arXiv preprint arXiv:2306.04642*, 2023. 1
- [11] Prafulla Dhariwal and Alexander Nichol. Diffusion models beat gans on image synthesis. *Advances in neural information processing systems*, 34:8780–8794, 2021. 1, 12
- [12] Patrick Esser, Robin Rombach, and Bjorn Ommer. Taming transformers for high-resolution image synthesis. In *Proceedings of the IEEE/CVF conference on computer vision and pattern recognition*, pages 12873–12883, 2021. 12
- [13] Patrick Esser, Sumith Kulal, Andreas Blattmann, Rahim Entezari, Jonas Müller, Harry Saini, Yam Levi, Dominik Lorenz, Axel Sauer, Frederic Boesel, et al. Scaling rectified flow transformers for high-resolution image synthesis. In *Forty-first International Conference on Machine Learning*, 2024. 1, 8
- [14] Junfeng Fang, Houcheng Jiang, Kun Wang, Yunshan Ma, Xiang Wang, Xiangnan He, and Tat-seng Chua. Alphaedit: Null-space constrained knowledge editing for language models. *arXiv preprint arXiv:2410.02355*, 2024. 2, 3, 8, 17
- [15] Chun-Mei Feng, Bangjun Li, Xinxing Xu, Yong Liu, Huazhu Fu, and Wangmeng Zuo. Learning federated visual prompt in null space for mri reconstruction. In *Proceedings of the IEEE/CVF Conference on Computer Vision and Pattern Recognition*, pages 8064–8073, 2023. 3
- [16] Rinon Gal, Yuval Alaluf, Yuval Atzmon, Or Patashnik, Amit H Bermano, Gal Chechik, and Daniel Cohen-Or. An image is worth one word: Personalizing text-to-image generation using textual inversion. *arXiv preprint arXiv:2208.01618*, 2022. 1
- [17] Rohit Gandikota, Joanna Materzynska, Jaden Fiotto-Kaufman, and David Bau. Erasing concepts from diffusion models. In *Proceedings of the IEEE/CVF International Conference on Computer Vision*, pages 2426–2436, 2023. 1, 2, 17
- [18] Rohit Gandikota, Hadas Orgad, Yonatan Belinkov, Joanna Materzynska, and David Bau. Unified concept editing in diffusion models. In *Proceedings of the IEEE/CVF Winter Conference on Applications of Computer Vision*, pages 5111–5120, 2024. 1, 2, 3, 4, 5, 6, 15, 16, 17
- [19] Chao Gong, Kai Chen, Zhipeng Wei, Jingjing Chen, and Yungang Jiang. Reliable and efficient concept erasure of text-to-image diffusion models. In *European Conference on Computer Vision*, pages 73–88. Springer, 2025. 1, 2, 3, 4, 5, 6, 7, 15, 16, 20
- [20] Nick Hasty, Ihor Kroosh, Dmitry Voitech, and Dmytro KorDuban. Giphy celebrity detector. <https://github.com/Giphy/celeb-detection-oss>. 6, 15
- [21] Amir Hertz, Ron Mokady, Jay Tenenbaum, Kfir Aberman, Yael Pritch, and Daniel Cohen-Or. Prompt-to-prompt image editing with cross attention control. *arXiv preprint arXiv:2208.01626*, 2022. 16
- [22] Martin Heusel, Hubert Ramsauer, Thomas Unterthiner, Bernhard Nessler, and Sepp Hochreiter. Gans trained by a two time-scale update rule converge to a local nash equilibrium. *Advances in neural information processing systems*, 30, 2017. 5
- [23] Jonathan Ho and Tim Salimans. Classifier-free diffusion guidance. *arXiv preprint arXiv:2207.12598*, 2022. 1, 5
- [24] Jonathan Ho, Ajay Jain, and Pieter Abbeel. Denoising diffusion probabilistic models. *Advances in neural information processing systems*, 33:6840–6851, 2020. 1, 12
- [25] Edward J Hu, Yelong Shen, Phillip Wallis, Zeyuan Allen-Zhu, Yuanzhi Li, Shean Wang, Lu Wang, and Weizhu Chen. Lora: Low-rank adaptation of large language models. *arXiv preprint arXiv:2106.09685*, 2021. 17

- [26] Diederik Kingma, Tim Salimans, Ben Poole, and Jonathan Ho. Variational diffusion models. *Advances in neural information processing systems*, 34:21696–21707, 2021. 12
- [27] Alexander Kirillov, Eric Mintun, Nikhila Ravi, Hanzi Mao, Chloe Rolland, Laura Gustafson, Tete Xiao, Spencer Whitehead, Alexander C Berg, Wan-Yen Lo, et al. Segment anything. In *Proceedings of the IEEE/CVF International Conference on Computer Vision*, pages 4015–4026, 2023. 8
- [28] Yajing Kong, Liu Liu, Zhen Wang, and Dacheng Tao. Balancing stability and plasticity through advanced null space in continual learning. In *European Conference on Computer Vision*, pages 219–236. Springer, 2022. 3
- [29] Nupur Kumari, Bingliang Zhang, Sheng-Yu Wang, Eli Shechtman, Richard Zhang, and Jun-Yan Zhu. Ablating concepts in text-to-image diffusion models. In *Proceedings of the IEEE/CVF International Conference on Computer Vision*, pages 22691–22702, 2023. 1, 2, 5, 15, 16
- [30] Ouxiang Li, Jiayin Cai, Yanbin Hao, Xiaolong Jiang, Yao Hu, and Fuli Feng. Improving synthetic image detection towards generalization: An image transformation perspective. *arXiv preprint arXiv:2408.06741*, 2024. 1
- [31] Ouxiang Li, Yanbin Hao, Zhicai Wang, Bin Zhu, Shuo Wang, Zaixi Zhang, and Fuli Feng. Model inversion attacks through target-specific conditional diffusion models. *arXiv preprint arXiv:2407.11424*, 2024. 1
- [32] Guoliang Lin, Hanlu Chu, and Hanjiang Lai. Towards better plasticity-stability trade-off in incremental learning: A simple linear connector. In *Proceedings of the IEEE/CVF conference on computer vision and pattern recognition*, pages 89–98, 2022. 3
- [33] Tsung-Yi Lin, Michael Maire, Serge Belongie, James Hays, Pietro Perona, Deva Ramanan, Piotr Dollár, and C Lawrence Zitnick. Microsoft coco: Common objects in context. In *Computer Vision—ECCV 2014: 13th European Conference, Zurich, Switzerland, September 6–12, 2014, Proceedings, Part V 13*, pages 740–755. Springer, 2014. 5, 15
- [34] Cheng Lu, Yuhao Zhou, Fan Bao, Jianfei Chen, Chongxuan Li, and Jun Zhu. Dpm-solver: A fast ode solver for diffusion probabilistic model sampling in around 10 steps. *Advances in Neural Information Processing Systems*, 35:5775–5787, 2022. 5
- [35] Shilin Lu, Zilan Wang, Leyang Li, Yanzhu Liu, and Adams Wai-Kin Kong. Mace: Mass concept erasure in diffusion models. In *Proceedings of the IEEE/CVF Conference on Computer Vision and Pattern Recognition*, pages 6430–6440, 2024. 1, 2, 5, 6, 15, 16, 17
- [36] Yue Lu, Shizhou Zhang, De Cheng, Yinghui Xing, Nannan Wang, Peng Wang, and Yanning Zhang. Visual prompt tuning in null space for continual learning. *arXiv preprint arXiv:2406.05658*, 2024. 3
- [37] Mengyao Lyu, Yuhong Yang, Haiwen Hong, Hui Chen, Xuan Jin, Yuan He, Hui Xue, Jungong Han, and Guiguang Ding. One-dimensional adapter to rule them all: Concepts diffusion models and erasing applications. In *Proceedings of the IEEE/CVF Conference on Computer Vision and Pattern Recognition*, pages 7559–7568, 2024. 1, 2, 4, 5, 15, 17
- [38] J MacQueen. Some methods for classification and analysis of multivariate observations. In *Proceedings of 5-th Berkeley Symposium on Mathematical Statistics and Probability/University of California Press*, 1967. 5
- [39] Alexander Quinn Nichol and Prafulla Dhariwal. Improved denoising diffusion probabilistic models. In *International conference on machine learning*, pages 8162–8171. PMLR, 2021. 1
- [40] OpenAI. OpenAI: Introducing ChatGPT, 2022. 15
- [41] OpenAI. Dall-e 3 system card. 2023. 2
- [42] Hadas Orgad, Bahjat Kawar, and Yonatan Belinkov. Editing implicit assumptions in text-to-image diffusion models. In *Proceedings of the IEEE/CVF International Conference on Computer Vision*, pages 7053–7061, 2023. 1, 3
- [43] William Peebles and Saining Xie. Scalable diffusion models with transformers. In *Proceedings of the IEEE/CVF International Conference on Computer Vision*, pages 4195–4205, 2023. 8
- [44] Dustin Podell, Zion English, Kyle Lacey, Andreas Blattmann, Tim Dockhorn, Jonas Müller, Joe Penna, and Robin Rombach. Sdxl: Improving latent diffusion models for high-resolution image synthesis. *arXiv preprint arXiv:2307.01952*, 2023. 1, 8
- [45] Alec Radford, Jong Wook Kim, Chris Hallacy, Aditya Ramesh, Gabriel Goh, Sandhini Agarwal, Girish Sastry, Amanda Askell, Pamela Mishkin, Jack Clark, et al. Learning transferable visual models from natural language supervision. In *International conference on machine learning*, pages 8748–8763. PMLR, 2021. 3, 5, 12, 15
- [46] Aditya Ramesh, Mikhail Pavlov, Gabriel Goh, Scott Gray, Chelsea Voss, Alec Radford, Mark Chen, and Ilya Sutskever. Zero-shot text-to-image generation. In *International conference on machine learning*, pages 8821–8831. Pmlr, 2021. 1
- [47] Javier Rando, Daniel Paleka, David Lindner, Lennart Heim, and Florian Tramèr. Red-teaming the stable diffusion safety filter. *arXiv preprint arXiv:2210.04610*, 2022. 2
- [48] Dana Rao. Responsible innovation in the age of generative ai, 2023. 2
- [49] Robin Rombach, Andreas Blattmann, Dominik Lorenz, Patrick Esser, and Björn Ommer. High-resolution image synthesis with latent diffusion models. In *Proceedings of the IEEE/CVF conference on computer vision and pattern recognition*, pages 10684–10695, 2022. 1, 2, 12
- [50] Nataniel Ruiz, Yuanzhen Li, Varun Jampani, Yael Pritch, Michael Rubinstein, and Kfir Aberman. Dreambooth: Fine tuning text-to-image diffusion models for subject-driven generation. In *Proceedings of the IEEE/CVF conference on computer vision and pattern recognition*, pages 22500–22510, 2023. 1
- [51] Patrick Schramowski, Manuel Brack, Björn Deiseroth, and Kristian Kersting. Safe latent diffusion: Mitigating inappropriate degeneration in diffusion models. In *Proceedings of the IEEE/CVF Conference on Computer Vision and Pattern Recognition*, pages 22522–22531, 2023. 1, 7, 17
- [52] Christoph Schuhmann, Richard Vencu, Romain Beaumont, Robert Kaczmarczyk, Clayton Mullis, Aarush Katta, Theo Coombes, Jenia Jitsev, and Aran Komatsuzaki. Laion-400m: Open dataset of clip-filtered 400 million image-text pairs. *arXiv preprint arXiv:2111.02114*, 2021. 2

- [53] Christoph Schuhmann, Romain Beaumont, Richard Vencu, Cade Gordon, Ross Wightman, Mehdi Cherti, Theo Coombes, Aarush Katta, Clayton Mullis, Mitchell Wortsman, et al. Laion-5b: An open large-scale dataset for training next generation image-text models. *Advances in Neural Information Processing Systems*, 35:25278–25294, 2022. [2](#)
- [54] Shawn Shan, Jenna Cryan, Emily Wenger, Haitao Zheng, Rana Hanocka, and Ben Y Zhao. Glaze: Protecting artists from style mimicry by {Text-to-Image} models. In *32nd USENIX Security Symposium (USENIX Security 23)*, pages 2187–2204, 2023. [1](#)
- [55] Jascha Sohl-Dickstein, Eric Weiss, Niru Maheswaranathan, and Surya Ganguli. Deep unsupervised learning using nonequilibrium thermodynamics. In *International Conference on Machine Learning*, pages 2256–2265. PMLR, 2015. [12](#)
- [56] Jiaming Song, Chenlin Meng, and Stefano Ermon. Denoising diffusion implicit models. *arXiv preprint arXiv:2010.02502*, 2020. [1](#)
- [57] Yang Song, Jascha Sohl-Dickstein, Diederik P Kingma, Abhishek Kumar, Stefano Ermon, and Ben Poole. Score-based generative modeling through stochastic differential equations. *arXiv preprint arXiv:2011.13456*, 2020. [1](#), [12](#)
- [58] Yoad Tewel, Rinon Gal, Gal Chechik, and Yuval Atzmon. Key-locked rank one editing for text-to-image personalization. In *ACM SIGGRAPH 2023 Conference Proceedings*, pages 1–11, 2023. [16](#)
- [59] Aaron Van Den Oord, Oriol Vinyals, et al. Neural discrete representation learning. *Advances in neural information processing systems*, 30, 2017. [12](#)
- [60] Shipeng Wang, Xiaorong Li, Jian Sun, and Zongben Xu. Training networks in null space of feature covariance for continual learning. In *Proceedings of the IEEE/CVF conference on Computer Vision and Pattern Recognition*, pages 184–193, 2021. [3](#)
- [61] Shipeng Wang, Xiaorong Li, Jian Sun, and Zongben Xu. Training networks in null space of feature covariance with self-supervision for incremental learning. *IEEE Transactions on Pattern Analysis and Machine Intelligence*, 2024. [3](#)
- [62] Yuan Wang, Ouxiang Li, Tingting Mu, Yanbin Hao, Kui Liu, Xiang Wang, and Xiangnan He. Precise, fast, and low-cost concept erasure in value space: Orthogonal complement matters. *arXiv preprint arXiv:2412.06143*, 2024. [16](#), [17](#)
- [63] Chengyi Yang, Mingda Dong, Xiaoyue Zhang, Jiayin Qi, and Aimin Zhou. Introducing common null space of gradients for gradient projection methods in continual learning. In *Proceedings of the 32nd ACM International Conference on Multimedia*, pages 5489–5497, 2024. [3](#)
- [64] Ling Yang, Zhilong Zhang, Yang Song, Shenda Hong, Runsheng Xu, Yue Zhao, Wentao Zhang, Bin Cui, and Ming-Hsuan Yang. Diffusion models: A comprehensive survey of methods and applications. *ACM Computing Surveys*, 56(4): 1–39, 2023. [1](#)
- [65] Yijun Yang, Ruiyuan Gao, Xiaosen Wang, Tsung-Yi Ho, Nan Xu, and Qiang Xu. Mma-diffusion: Multimodal attack on diffusion models. In *Proceedings of the IEEE/CVF Conference on Computer Vision and Pattern Recognition*, pages 7737–7746, 2024. [1](#)
- [66] Gong Zhang, Kai Wang, Xingqian Xu, Zhangyang Wang, and Humphrey Shi. Forget-me-not: Learning to forget in text-to-image diffusion models. In *Proceedings of the IEEE/CVF Conference on Computer Vision and Pattern Recognition*, pages 1755–1764, 2024. [1](#), [2](#), [17](#)
- [67] Yimeng Zhang, Jinghan Jia, Xin Chen, Aochuan Chen, Yihua Zhang, Jiancheng Liu, Ke Ding, and Sijia Liu. To generate or not? safety-driven unlearned diffusion models are still easy to generate unsafe images... for now. In *European Conference on Computer Vision*, pages 385–403. Springer, 2025. [1](#)

## A. Preliminaries

**T2I diffusion models.** T2I generation has seen significant advancements with diffusion models, particularly Latent Diffusion Models (LDMs) [49]. Unlike pixel-space diffusion, LDMs operate in the latent space of a pretrained autoencoder, reducing computational costs while maintaining high-quality synthesis. LDMs consist of a vector-quantized autoencoder [12, 59] and a diffusion model [11, 24, 26, 55, 57]. The autoencoder encodes an image  $\mathbf{x}$  into a latent representation  $\mathbf{z} = \mathcal{E}(\mathbf{x})$  and reconstructs it via  $\mathbf{x} \approx \mathcal{D}(\mathbf{z})$ . The diffusion model learns to generate latent codes through a denoising process. The training objective is given by [24, 49]:

$$\mathcal{L}_{\text{LDM}} = \mathbb{E}_{\mathbf{z} \sim \mathcal{E}(\mathbf{x}), \mathbf{c}, \epsilon \sim \mathcal{N}(0,1), t} \left[ \|\epsilon - \epsilon_{\theta}(\mathbf{z}_t, t, \mathbf{c})\|_2^2 \right], \quad (13)$$

where  $\mathbf{z}_t$  is the noisy latent at timestep  $t$ ,  $\epsilon$  is Gaussian noise,  $\epsilon_{\theta}$  is the denoising network, and  $\mathbf{c}$  is conditioning information from text, class labels, or segmentation masks [49]. During inference, a latent  $\mathbf{z}_T$  is sampled from a Gaussian prior and progressively denoised to obtain  $\mathbf{z}_0$ , which is then decoded into an image via  $\mathbf{x}_0 \approx \mathcal{D}(\mathbf{z}_0)$ .

**Cross-attention mechanisms.** Current T2I diffusion models usually leverage a generative framework to synthesize images conditioned on textual descriptions in latent space [49]. The conditioning mechanism is implemented through cross-attention (CA) layers. Specifically, textual descriptions are first tokenized into  $n$  tokens and embedded into a sequence of vectors  $\mathbf{e} \in \mathbb{R}^{d_0 \times n}$  via a pre-trained CLIP model [45]. These text embeddings serve as the key  $\mathbf{K} \in \mathbb{R}^{n \times d_k}$  and value  $\mathbf{V} \in \mathbb{R}^{n \times d_v}$  inputs using parametric projection matrices  $\mathbf{W}_{\mathbf{K}} \in \mathbb{R}^{d_k \times d_0}$  and  $\mathbf{W}_{\mathbf{V}} \in \mathbb{R}^{d_v \times d_0}$ , while the intermediate image representations act as the query  $\mathbf{Q} \in \mathbb{R}^{m \times d_k}$ . The cross-attention mechanism is defined as:

$$\text{Attention}(\mathbf{Q}, \mathbf{K}, \mathbf{V}) = \text{softmax} \left( \frac{\mathbf{Q}\mathbf{K}^T}{\sqrt{d_k}} \right) \mathbf{V}. \quad (14)$$

This alignment enables the model to capture semantic correlations between the textual input and the visual features, ensuring that the generated images are semantically consistent with the provided text prompts.

## B. Proof and Derivation

### B.1. Deriving the Closed-Form Solution for UCE

From Eq. 1, we are tasked with minimizing the following editing objective, where the hyperparameters  $\alpha$  and  $\beta$  correspond to the weights of the erasure error  $e_1$  and the preservation error  $e_0$ , respectively:

$$\min_{\Delta} [\alpha \|\mathbf{W} + \Delta\| \mathbf{C}_1 - \mathbf{W}\mathbf{C}_* \|^2 + \beta \|\Delta\mathbf{C}_0\|^2]. \quad (15)$$

To derive the closed-form solution, we begin by computing the gradient of the objective function with respect to  $\Delta$ . The gradient is given by:

$$\alpha (\mathbf{W}\mathbf{C}_1 - \mathbf{W}\mathbf{C}_* + \Delta\mathbf{C}_1) \mathbf{C}_1^T + \beta \Delta\mathbf{C}_0\mathbf{C}_0^T = 0. \quad (16)$$

Solving the resulting equation yields the closed-form solution for  $\Delta_{\text{UCE}}$ :

$$\Delta_{\text{UCE}} = \alpha \mathbf{W} (\mathbf{C}_*\mathbf{C}_1^T - \mathbf{C}_1\mathbf{C}_1^T) (\alpha\mathbf{C}_1\mathbf{C}_1^T + \beta\mathbf{C}_0\mathbf{C}_0^T)^{-1}. \quad (17)$$

In practice, an additional identity matrix  $\mathbf{I}$  with hyperparameter  $\lambda$  is added to  $(\alpha\mathbf{C}_1\mathbf{C}_1^T + \beta\mathbf{C}_0\mathbf{C}_0^T)^{-1}$  to ensure its invertibility. This modification results in the following closed-form solution for UCE:

$$\Delta_{\text{UCE}} = \alpha \mathbf{W} (\mathbf{C}_*\mathbf{C}_1^T - \mathbf{C}_1\mathbf{C}_1^T) (\alpha\mathbf{C}_1\mathbf{C}_1^T + \beta\mathbf{C}_0\mathbf{C}_0^T + \lambda\mathbf{I})^{-1}. \quad (18)$$

### B.2. Proof of the Lower Bound of $e_0$ for UCE

Herein, we aim to establish the existence of a strictly positive constant  $c > 0$  such that

$$e_0 = \|\Delta_{\text{UCE}}\mathbf{C}_0\|^2 = \|\alpha \mathbf{W} (\mathbf{C}_*\mathbf{C}_1^T - \mathbf{C}_1\mathbf{C}_1^T) (\alpha\mathbf{C}_1\mathbf{C}_1^T + \beta\mathbf{C}_0\mathbf{C}_0^T + \lambda\mathbf{I})^{-1}\mathbf{C}_0\|^2 \geq c > 0. \quad (19)$$

**Assumption B.1.** We assume that  $\alpha, \beta, \lambda \neq 0$ , that  $\mathbf{W}$  is a full-rank matrix, and that  $\mathbf{C}_0\mathbf{C}_0^T$  is rank-deficient. Furthermore, we assume that

$$\mathbf{C}_*\mathbf{C}_1^T - \mathbf{C}_1\mathbf{C}_1^T \neq \mathbf{0}.$$

*Proof.* Define the matrix  $\mathbf{M}$  as

$$\mathbf{M} = \alpha \mathbf{C}_1 \mathbf{C}_1^\top + \beta \mathbf{C}_0 \mathbf{C}_0^\top + \lambda \mathbf{I}. \quad (20)$$

Since  $\lambda > 0$  and  $\mathbf{I}$  is positive definite, it follows that  $\mathbf{M}$  is strictly positive definite and therefore invertible.

Rewriting  $e_0$  by defining  $\mathbf{B} = \mathbf{M}^{-1} \mathbf{C}_0$ , we obtain

$$e_0 = \|\alpha \mathbf{W}(\mathbf{C}_* \mathbf{C}_1^\top - \mathbf{C}_1 \mathbf{C}_1^\top) \mathbf{B}\|^2. \quad (21)$$

Applying the singular value bound for matrix products, we have

$$\|\mathbf{X}\mathbf{Y}\| \geq \sigma_{\min}(\mathbf{X})\|\mathbf{Y}\|, \quad (22)$$

where  $\sigma_{\min}(\mathbf{X})$  is the smallest singular value of  $\mathbf{X}$ . Applying this inequality, we obtain

$$\|\mathbf{W}(\mathbf{C}_* \mathbf{C}_1^\top - \mathbf{C}_1 \mathbf{C}_1^\top) \mathbf{B}\| \geq \sigma_{\min}(\mathbf{W})\|(\mathbf{C}_* \mathbf{C}_1^\top - \mathbf{C}_1 \mathbf{C}_1^\top) \mathbf{B}\|. \quad (23)$$

We start with the singular value decomposition (SVD) of the matrix  $\mathbf{C}_* \mathbf{C}_1^\top - \mathbf{C}_1 \mathbf{C}_1^\top$ , given by

$$\mathbf{C}_* \mathbf{C}_1^\top - \mathbf{C}_1 \mathbf{C}_1^\top = \mathbf{U} \mathbf{\Sigma} \mathbf{V}^\top. \quad (24)$$

Here,  $\mathbf{U}$  and  $\mathbf{V}$  are orthogonal matrices, and

$$\mathbf{\Sigma} = \text{diag}(\sigma_1, \sigma_2, \dots, \sigma_r, 0, \dots, 0) \quad (25)$$

is a diagonal matrix containing the singular values  $\sigma_1 \geq \sigma_2 \geq \dots \geq \sigma_r > 0$ , followed by zeros.

Multiplying both sides by  $\mathbf{B}$ , we obtain

$$(\mathbf{C}_* \mathbf{C}_1^\top - \mathbf{C}_1 \mathbf{C}_1^\top) \mathbf{B} = \mathbf{U} \mathbf{\Sigma} \mathbf{V}^\top \mathbf{B}. \quad (26)$$

Define the projection of  $\mathbf{B}$  onto the subspace spanned by the first  $r$  right singular vectors (corresponding to the nonzero singular values) as

$$\mathbf{B}_{\text{proj}} = \mathbf{V}_r^\top \mathbf{B}, \quad (27)$$

where  $\mathbf{V}_r$  consists of the first  $r$  columns of  $\mathbf{V}$ . Then, we can rewrite the expression as

$$(\mathbf{C}_* \mathbf{C}_1^\top - \mathbf{C}_1 \mathbf{C}_1^\top) \mathbf{B} = \mathbf{U} \mathbf{\Sigma} \mathbf{B}_{\text{proj}}. \quad (28)$$

Taking norms on both sides and using the fact that orthogonal transformations preserve norms, we get

$$\|(\mathbf{C}_* \mathbf{C}_1^\top - \mathbf{C}_1 \mathbf{C}_1^\top) \mathbf{B}\| = \|\mathbf{\Sigma} \mathbf{B}_{\text{proj}}\|. \quad (29)$$

Since  $\mathbf{\Sigma}$  is a diagonal matrix, its smallest nonzero singular value  $\sigma_r$  provides a lower bound:

$$\|\mathbf{\Sigma} \mathbf{B}_{\text{proj}}\| \geq \sigma_r \|\mathbf{B}_{\text{proj}}\|. \quad (30)$$

Next, we establish a lower bound for  $\|\mathbf{B}_{\text{proj}}\|$ . Since  $\mathbf{B}$  is not entirely in the null space of  $\mathbf{C}_* \mathbf{C}_1^\top - \mathbf{C}_1 \mathbf{C}_1^\top$  (by assumption that the matrix is nonzero), there exists a constant  $c_1 > 0$  such that

$$\|\mathbf{B}_{\text{proj}}\| \geq c_1 \|\mathbf{B}\|. \quad (31)$$

Combining these inequalities, we obtain

$$\|(\mathbf{C}_* \mathbf{C}_1^\top - \mathbf{C}_1 \mathbf{C}_1^\top) \mathbf{B}\| \geq \sigma_r \|\mathbf{B}_{\text{proj}}\| \geq \sigma_r c_1 \|\mathbf{B}\|. \quad (32)$$

Since  $\mathbf{M}$  is positive definite, we use the standard norm inequality for an invertible matrix  $\mathbf{M}$ , which states that for any matrix  $\mathbf{X}$ ,

$$\|\mathbf{M}\mathbf{X}\| \leq \|\mathbf{M}\| \|\mathbf{X}\|. \quad (33)$$

Setting  $\mathbf{X} = \mathbf{M}^{-1} \mathbf{C}_0$ , we obtain

$$\|\mathbf{M}\mathbf{M}^{-1} \mathbf{C}_0\| \leq \|\mathbf{M}\| \|\mathbf{M}^{-1} \mathbf{C}_0\|. \quad (34)$$

Since  $\mathbf{M}\mathbf{M}^{-1} = \mathbf{I}$ , the left-hand side simplifies to  $\|\mathbf{C}_0\|$ , yielding

$$\|\mathbf{C}_0\| \leq \|\mathbf{M}\| \|\mathbf{M}^{-1}\mathbf{C}_0\|. \quad (35)$$

Dividing both sides by  $\|\mathbf{M}\|$ , we obtain

$$\|\mathbf{M}^{-1}\mathbf{C}_0\| \geq \frac{1}{\|\mathbf{M}\|} \|\mathbf{C}_0\|. \quad (36)$$

Thus, it follows that

$$\|\mathbf{B}\| = \|\mathbf{M}^{-1}\mathbf{C}_0\| \geq \frac{1}{\|\mathbf{M}\|} \|\mathbf{C}_0\|. \quad (37)$$

Combining the above results, we obtain

$$\|\mathbf{W}(\mathbf{C}_* \mathbf{C}_1^\top - \mathbf{C}_1 \mathbf{C}_1^\top) \mathbf{B}\| \geq \sigma_{\min}(\mathbf{W}) \sigma_r c_1 \frac{1}{\|\mathbf{M}\|} \|\mathbf{C}_0\|. \quad (38)$$

Squaring both sides, we conclude that

$$e_0 = \|\alpha \mathbf{W}(\mathbf{C}_* \mathbf{C}_1^\top - \mathbf{C}_1 \mathbf{C}_1^\top) \mathbf{B}\|^2 \geq \alpha^2 \sigma_{\min}^2(\mathbf{W}) \sigma_r^2 c_1^2 \frac{1}{\|\mathbf{M}\|^2} \|\mathbf{C}_0\|^2. \quad (39)$$

Since all terms on the right-hand side are strictly positive by assumption, we establish the existence of a positive lower bound  $c > 0$  such that

$$e_0 \geq c > 0. \quad (40)$$

This completes the proof.  $\square$

### B.3. Deriving the Closed-Form Solution for Ours

From Eq. 9, we are tasked with minimizing the following editing objective:

$$\min_{\Delta} \|(\mathbf{W} + \Delta \mathbf{P})\mathbf{C}_1 - \mathbf{W}\mathbf{C}_*\|^2 + \|\Delta \mathbf{P}\|^2, \quad \text{s.t. } (\Delta \mathbf{P})\mathbf{C}_2 = \mathbf{0}. \quad (41)$$

This is a weighted least squares problem subject to an equality constraint. To solve it, we first formulate the Lagrangian function, where  $\Lambda$  is the Lagrange multiplier:

$$\mathcal{L}(\Delta, \Lambda) = \|(\mathbf{W} + \Delta \mathbf{P})\mathbf{C}_1 - \mathbf{W}\mathbf{C}_*\|^2 + \|\Delta \mathbf{P}\|^2 + \Lambda^\top ((\Delta \mathbf{P})\mathbf{C}_2). \quad (42)$$

We compute the gradient of the Lagrangian function in Eq. 42 with respect to  $\Delta$  and set it to zero, yielding the following equation for  $\Delta$ :

$$\frac{\partial \mathcal{L}(\Delta, \Lambda)}{\partial \Delta} = 2((\mathbf{W} + \Delta \mathbf{P})\mathbf{C}_1 - \mathbf{W}\mathbf{C}_*) \mathbf{C}_1^\top \mathbf{P}^\top + 2\Delta \mathbf{P} \mathbf{P}^\top + \Lambda \mathbf{C}_2^\top \mathbf{P}^\top = \mathbf{0}. \quad (43)$$

Given that the projection matrix  $\mathbf{P}$  is derived from  $R_{\text{refine}}$  using Eq. 2,  $\mathbf{P}$  is a symmetric matrix (*i.e.*,  $\mathbf{P} = \mathbf{P}^\top$ ) and an idempotent matrix (*i.e.*,  $\mathbf{P}^2 = \mathbf{P}$ ), the above formulation can be simplified to:

$$\frac{\partial \mathcal{L}(\Delta, \Lambda)}{\partial \Delta} = 2((\mathbf{W} + \Delta \mathbf{P})\mathbf{C}_1 - \mathbf{W}\mathbf{C}_*) \mathbf{C}_1^\top \mathbf{P} + 2\Delta \mathbf{P} + \Lambda \mathbf{C}_2^\top \mathbf{P} = \mathbf{0}. \quad (44)$$

Therefore, we can obtain the closed-form solution for  $\Delta \mathbf{P}$  from this equation:

$$\Delta \mathbf{P} = (\mathbf{W}\mathbf{C}_* \mathbf{C}_1^\top \mathbf{P} - \mathbf{W}\mathbf{C}_1 \mathbf{C}_1^\top \mathbf{P} - \frac{1}{2} \Lambda \mathbf{C}_2^\top \mathbf{P})(\mathbf{C}_1 \mathbf{C}_1^\top \mathbf{P} + \mathbf{I})^{-1}. \quad (45)$$

Next, we differentiate the Lagrangian function in Eq. 42 with respect to  $\Lambda$  and set it to zero:

$$\frac{\partial \mathcal{L}(\Delta, \Lambda)}{\partial \Lambda} = (\Delta \mathbf{P})\mathbf{C}_2 = \mathbf{0}. \quad (46)$$

For simplicity, we define  $\mathbf{M} = (\mathbf{C}_1 \mathbf{C}_1^\top \mathbf{P} + \mathbf{I})^{-1}$ . Then, we substitute the result of Eq. 45 into Eq. 46 and obtain:

$$(\mathbf{W}\mathbf{C}_* \mathbf{C}_1^\top \mathbf{P} - \mathbf{W}\mathbf{C}_1 \mathbf{C}_1^\top \mathbf{P} - \frac{1}{2} \Lambda \mathbf{C}_2^\top \mathbf{P}) \mathbf{M} \mathbf{C}_2 = \mathbf{0}. \quad (47)$$

Solving this equation leads to:

$$\frac{1}{2}\Lambda = \mathbf{W}(\mathbf{C}_* \mathbf{C}_1^\top - \mathbf{C}_1 \mathbf{C}_1^\top) \mathbf{P} \mathbf{M} \mathbf{C}_2 (\mathbf{C}_2^\top \mathbf{P} \mathbf{M} \mathbf{C}_2)^{-1}. \quad (48)$$

Substituting Eq.48 back into Eq.45, we have the closed-form solution of our objective:

$$(\Delta \mathbf{P})_{\text{SPEED}} = \mathbf{W}(\mathbf{C}_* \mathbf{C}_1^\top - \mathbf{C}_1 \mathbf{C}_1^\top) \mathbf{P} \mathbf{Q} \mathbf{M}, \quad (49)$$

where  $\mathbf{Q} = \mathbf{I} - \mathbf{M} \mathbf{C}_2 (\mathbf{C}_2^\top \mathbf{P} \mathbf{M} \mathbf{C}_2)^{-1} \mathbf{C}_2^\top \mathbf{P}$  and  $\mathbf{M} = (\mathbf{C}_1 \mathbf{C}_1^\top \mathbf{P} + \mathbf{I})^{-1}$ .

## C. Implementation Details

### C.1. Experimental Setup Details

**Few-concept erasure.** We first compare methods on few-concept erasure, a fundamental concept erasure task, including both instance erasure and artistic style erasure following [37]. For instance erasure, we prepare 80 instance templates proposed in CLIP [45], such as “a photo of the {Instance}”, “a drawing of the {Instance}”, and “a painting of the {Instance}”. For artistic style erasure, we use ChatGPT [5, 40] to generate 30 artistic style templates, including “{Artistic} style painting of the night sky with bold strokes”, “{Artistic} style landscape of rolling hills with dramatic brushwork”, and “Sunrise scene in {Artistic} style, capturing the beauty of dawn”. Following [37], we handpick the representative target and anchor concepts as the erasure set (i.e., *Snoopy, Mickey, SpongeBob* → ‘ ’ in instance erasure and *Van Gogh, Picasso, Monet* → ‘art’ in artistic style erasure) and non-target concepts for evaluation (i.e., *Pikachu* and *Hello Kitty* in instance erasure and *Paul Gauguin* and *Caravaggio* in artistic style erasure). In terms of the retain set, for instance erasure, we use a scraping script to crawl Wikipedia category pages to extract fictional character names and their page view counts with a threshold of 500,000 views from 2020.01.01 to 2023.12.31, resulting in 1,352 instances. For artistic style erasure, we use the 1,734 artistic styles collected from UCE [18]. In evaluation, we generate 10 images per template per concept, resulting in 800 and 300 images for each concept in instance erasure and artistic style erasure, respectively. Moreover, we introduce the MS-COCO captions [33] to serve as general prior knowledge. In implementation, we use the first 1,000 captions to generate a total of 1000 images to compare CS and FID before and after erasure.

**Multi-concept erasure.** We then compare methods on multi-concept erasure, a more challenging and realistic concept erasure task. Following the experiment setup from [35], we introduce a dataset consisting of 200 celebrities, where their portraits generated by SDv1.4 [1] can be recognizable with exceptional accuracy by the GIPHY Celebrity Detector (GCD) [20]. This dataset is divided into two groups: an erasure set with 10, 50, and 100 celebrities and a retain set with 100 other celebrities. The full list for both sets is presented in Table 7. We experiment with erasing 10, 50, and 100 celebrities with the pre-defined target concepts and the entire retain set is utilized in all cases. In evaluation, we prepare five celebrity templates, (i.e., “a portrait of {Celebrity}”, “a sketch of {Celebrity}”, “an oil painting of {Celebrity}”, “{Celebrity} in an official photo”, and “an image capturing {Celebrity} at a public event”) and generate 500 images for both sets. For non-target concepts, we generate 1 image per template for each of the 100 concepts, totaling 500 images. For target concepts, we adjust the per-concept quantity to maintain a total of 500 images (e.g., erasing 10 celebrities involves generating 10 images with 5 templates).

**Implicit concept erasure.** We adopt the same setting in [19] to erase *nudity* → ‘ ’ as the erasure set and ‘ ’ as the retain set. In evaluation, we generate images using all 4,703 prompts in I2P and use NudeNet [6] to identify nude content with the threshold of 0.6.

### C.2. Erasure Configurations

**Implementation of previous works.** In our series of three concept erasure tasks, we mainly compare against four methods: ConAbl<sup>‡</sup> [29], MACE<sup>§</sup> [35], RECE<sup>¶</sup> [19], and UCE<sup>||</sup> [18], as they achieve SOTA performance across different concept erasure tasks. All the compared methods are implemented using their default configurations from the corresponding official repositories. One exception is that for MACE when erasing 50 celebrities, since it doesn’t provide an official configuration and the *preserve weight* varies with the number of target celebrities, we set it to  $1.2 \times 10^5$  to ensure a consistent balance between erasure and preservation.

<sup>‡</sup><https://github.com/nupurkmr9/concept-ablation>

<sup>§</sup><https://github.com/Shilin-LU/MACE>

<sup>¶</sup><https://github.com/CharlesGong12/RECE>

<sup>||</sup><https://github.com/rohitgandikota/unified-concept-editing>

| Group       | Number          | Anchor Concept | Celebrity                                                                                                                                                                                                                                                                                                                                                                                                                                                                                                                                                                                                                                                                                                                                                                                                                                                                                                                                                                                                                                                                                                                                                                                                                                                                                                                                                                                                                                                                                                                                                                                                                                                                                                           |
|-------------|-----------------|----------------|---------------------------------------------------------------------------------------------------------------------------------------------------------------------------------------------------------------------------------------------------------------------------------------------------------------------------------------------------------------------------------------------------------------------------------------------------------------------------------------------------------------------------------------------------------------------------------------------------------------------------------------------------------------------------------------------------------------------------------------------------------------------------------------------------------------------------------------------------------------------------------------------------------------------------------------------------------------------------------------------------------------------------------------------------------------------------------------------------------------------------------------------------------------------------------------------------------------------------------------------------------------------------------------------------------------------------------------------------------------------------------------------------------------------------------------------------------------------------------------------------------------------------------------------------------------------------------------------------------------------------------------------------------------------------------------------------------------------|
| Erasure Set | 10              | 'person'       | 'Adam Driver', 'Adriana Lima', 'Amber Heard', 'Amy Adams', 'Andrew Garfield', 'Angelina Jolie', 'Anjelica Huston', 'Anna Faris', 'Anna Kendrick', 'Anne Hathaway'                                                                                                                                                                                                                                                                                                                                                                                                                                                                                                                                                                                                                                                                                                                                                                                                                                                                                                                                                                                                                                                                                                                                                                                                                                                                                                                                                                                                                                                                                                                                                   |
|             | 50              | 'person'       | 'Adam Driver', 'Adriana Lima', 'Amber Heard', 'Amy Adams', 'Andrew Garfield', 'Angelina Jolie', 'Anjelica Huston', 'Anna Faris', 'Anna Kendrick', 'Anne Hathaway', 'Arnold Schwarzenegger', 'Barack Obama', 'Beth Behrs', 'Bill Clinton', 'Bob Dylan', 'Bob Marley', 'Bradley Cooper', 'Bruce Willis', 'Bryan Cranston', 'Cameron Diaz', 'Channing Tatum', 'Charlie Sheen', 'Charlize Theron', 'Chris Evans', 'Chris Hemsworth', 'Chris Pine', 'Chuck Norris', 'Courteney Cox', 'Demi Lovato', 'Drake', 'Drew Barrymore', 'Dwayne Johnson', 'Ed Sheeran', 'Elon Musk', 'Elvis Presley', 'Emma Stone', 'Frida Kahlo', 'George Clooney', 'Glenn Close', 'Gwyneth Paltrow', 'Harrison Ford', 'Hillary Clinton', 'Hugh Jackman', 'Idris Elba', 'Jake Gyllenhaal', 'James Franco', 'Jared Leto', 'Jason Momoa', 'Jennifer Aniston', 'Jennifer Lawrence'                                                                                                                                                                                                                                                                                                                                                                                                                                                                                                                                                                                                                                                                                                                                                                                                                                                                  |
|             | 100             | 'person'       | 'Adam Driver', 'Adriana Lima', 'Amber Heard', 'Amy Adams', 'Andrew Garfield', 'Angelina Jolie', 'Anjelica Huston', 'Anna Faris', 'Anna Kendrick', 'Anne Hathaway', 'Arnold Schwarzenegger', 'Barack Obama', 'Beth Behrs', 'Bill Clinton', 'Bob Dylan', 'Bob Marley', 'Bradley Cooper', 'Bruce Willis', 'Bryan Cranston', 'Cameron Diaz', 'Channing Tatum', 'Charlie Sheen', 'Charlize Theron', 'Chris Evans', 'Chris Hemsworth', 'Chris Pine', 'Chuck Norris', 'Courteney Cox', 'Demi Lovato', 'Drake', 'Drew Barrymore', 'Dwayne Johnson', 'Ed Sheeran', 'Elon Musk', 'Elvis Presley', 'Emma Stone', 'Frida Kahlo', 'George Clooney', 'Glenn Close', 'Gwyneth Paltrow', 'Harrison Ford', 'Hillary Clinton', 'Hugh Jackman', 'Idris Elba', 'Jake Gyllenhaal', 'James Franco', 'Jared Leto', 'Jason Momoa', 'Jennifer Aniston', 'Jennifer Lawrence', 'Jennifer Lopez', 'Jeremy Renner', 'Jessica Biel', 'Jessica Chastain', 'John Oliver', 'John Wayne', 'Johnny Depp', 'Julianne Hough', 'Justin Timberlake', 'Kate Winslet', 'Leonardo DiCaprio', 'Margot Robbie', 'Mariah Carey', 'Melania Trump', 'Meryl Streep', 'Mick Jagger', 'Mila Kunis', 'Milla Jovovich', 'Morgan Freeman', 'Nick Jonas', 'Nicolas Cage', 'Nicole Kidman', 'Octavia Spencer', 'Olivia Wilde', 'Oprah Winfrey', 'Paul McCartney', 'Paul Walker', 'Peter Dinklage', 'Philip Seymour Hoffman', 'Reese Witherspoon', 'Richard Gere', 'Ricky Gervais', 'Rihanna', 'Robin Williams', 'Ronald Reagan', 'Ryan Gosling', 'Ryan Reynolds', 'Shia Labeouf', 'Shirley Temple', 'Spike Lee', 'Stan Lee', 'Theresa May', 'Tom Cruise', 'Tom Hanks', 'Tom Hardy', 'Tom Hiddleston', 'Whoopi Goldberg', 'Zac Efron', 'Zayn Malik'                         |
| Retain Set  | 10, 50, and 100 | -              | 'Aaron Paul', 'Alec Baldwin', 'Amanda Seyfried', 'Amy Poehler', 'Amy Schumer', 'Amy Winehouse', 'Andy Samberg', 'Aretha Franklin', 'Avril Lavigne', 'Aziz Ansari', 'Barry Manilow', 'Ben Affleck', 'Ben Stiller', 'Benicio Del Toro', 'Bette Midler', 'Betty White', 'Bill Murray', 'Bill Nye', 'Britney Spears', 'Brittany Snow', 'Bruce Lee', 'Burt Reynolds', 'Charles Manson', 'Christie Brinkley', 'Christina Hendricks', 'Clint Eastwood', 'Countess Vaughn', 'Dakota Johnson', 'Dane DeHaan', 'David Bowie', 'David Tennant', 'Denise Richards', 'Doris Day', 'Dr Dre', 'Elizabeth Taylor', 'Emma Roberts', 'Fred Rogers', 'Gal Gadot', 'George Bush', 'George Takei', 'Gillian Anderson', 'Gordon Ramsey', 'Halle Berry', 'Harry Dean Stanton', 'Harry Styles', 'Hayley Atwell', 'Heath Ledger', 'Henry Cavill', 'Jackie Chan', 'Jada Pinkett Smith', 'James Garner', 'Jason Statham', 'Jeff Bridges', 'Jennifer Connelly', 'Jensen Ackles', 'Jim Morrison', 'Jimmy Carter', 'Joan Rivers', 'John Lennon', 'Johnny Cash', 'Jon Hamm', 'Judy Garland', 'Julianne Moore', 'Justin Bieber', 'Kaley Cuoco', 'Kate Upton', 'Keanu Reeves', 'Kim Jong Un', 'Kirsten Dunst', 'Kristen Stewart', 'Krysten Ritter', 'Lana Del Rey', 'Leslie Jones', 'Lily Collins', 'Lindsay Lohan', 'Liv Tyler', 'Lizzy Caplan', 'Maggie Gyllenhaal', 'Matt Damon', 'Matt Smith', 'Matthew McConaughey', 'Maya Angelou', 'Megan Fox', 'Mel Gibson', 'Melanie Griffith', 'Michael Cera', 'Michael Ealy', 'Natalie Portman', 'Neil Degrasse Tyson', 'Niall Horan', 'Patrick Stewart', 'Paul Rudd', 'Paul Wesley', 'Pierce Brosnan', 'Prince', 'Queen Elizabeth', 'Rachel Dratch', 'Rachel McAdams', 'Reba McEntire', 'Robert De Niro' |

Table 7. **The evaluation setup for multi-concept erasure.** This celebrity dataset contains an erasure set with 100 celebrities and a retain set with another 100 celebrities. We experiment with erasing 10, 50, and 100 celebrities with the pre-defined target concepts and the entire retain set is utilized in all cases.

**Implementation of SPEED.** In line with previous methods [18, 19, 29, 35], we edit the cross-attention (CA) layers within the diffusion model due to their role in text-image alignment [21]. In contrast, we only edit the value matrices in the CA layers, as suggested by [62]. This choice is grounded in the observation that the keys in CA layers typically govern the layout and compositional structure of the attention map, while the values control the content and visual appearance of the images [58]. In the context of concept erasure, our goal is to effectively remove the semantics of the target concept, and we find that only editing the value matrices is sufficient as shown in Fig. 5 and 6 (further ablation comparison is provided in Appx. D.3). The augmentation times  $N_A$  in Eq. 8 is set to 10 and the augmentation ranks  $r$  in Eq. 6 is set to 1 as ablated in Appx. D.3. Meanwhile, given that eigenvalues are rarely strictly zero in practical applications when determining the null

|                                                            | <i>Snoopy</i> |        | <i>Mickey</i> |              | <i>Spongebob</i> |              | <i>Pikachu</i> |              | <i>Hello Kitty</i> |              | <i>MS-COCO</i> |              |
|------------------------------------------------------------|---------------|--------|---------------|--------------|------------------|--------------|----------------|--------------|--------------------|--------------|----------------|--------------|
|                                                            | CS            | FID    | CS            | FID          | CS               | FID          | CS             | FID          | CS                 | FID          | CS             | FID          |
| SD v1.4                                                    | 28.51         | -      | 26.62         | -            | 27.30            | -            | 27.44          | -            | 27.77              | -            | 26.53          | -            |
| Erase <i>Snoopy</i>                                        |               |        |               |              |                  |              |                |              |                    |              |                |              |
|                                                            | CS ↓          | FID ↑  | CS ↑          | FID ↓        | CS ↑             | FID ↓        | CS ↑           | FID ↓        | CS ↑               | FID ↓        | CS ↑           | FID ↓        |
| ConAbl                                                     | 25.44         | 98.38  | 26.63         | 37.08        | 26.95            | 38.92        | 27.47          | 26.14        | 27.65              | 36.52        | 26.40          | 21.20        |
| MACE                                                       | 20.90         | 165.74 | 23.46         | 105.97       | 23.35            | 102.77       | 26.05          | 65.71        | 26.05              | 75.42        | 26.09          | 42.62        |
| RECE                                                       | <b>18.38</b>  | 151.46 | 26.62         | 26.63        | 27.23            | 34.42        | 27.47          | 21.99        | 27.78              | 32.35        | 26.39          | 25.61        |
| UCE                                                        | 23.19         | 102.86 | 26.64         | 24.87        | 27.29            | 29.86        | 27.47          | 19.06        | 27.75              | 27.86        | 26.46          | 22.18        |
| Ours                                                       | 23.50         | 108.51 | 26.67         | <b>23.41</b> | 27.31            | <b>24.64</b> | 27.48          | <b>16.81</b> | <b>27.82</b>       | <b>21.74</b> | <b>26.48</b>   | <b>19.95</b> |
| Erase <i>Snoopy</i> and <i>Mickey</i>                      |               |        |               |              |                  |              |                |              |                    |              |                |              |
|                                                            | CS ↓          | FID ↑  | CS ↓          | FID ↑        | CS ↑             | FID ↓        | CS ↑           | FID ↓        | CS ↑               | FID ↓        | CS ↑           | FID ↓        |
| ConAbl                                                     | 25.26         | 106.78 | 26.58         | 57.05        | 26.81            | 45.08        | 27.34          | 35.57        | 27.74              | 41.48        | 26.42          | 24.34        |
| MACE                                                       | 20.53         | 170.01 | 20.63         | 142.98       | 22.03            | 112.01       | 24.98          | 91.72        | 23.64              | 106.88       | 25.50          | 55.15        |
| RECE                                                       | <b>18.57</b>  | 150.84 | <b>19.14</b>  | 145.59       | 27.29            | 35.85        | 27.37          | 26.05        | 27.71              | 40.77        | 26.31          | 30.30        |
| UCE                                                        | 23.60         | 99.30  | 24.79         | 86.32        | 27.32            | 30.58        | 27.38          | 23.51        | 27.74              | 31.76        | 26.38          | 26.06        |
| Ours                                                       | 23.58         | 103.62 | 23.62         | 83.70        | 27.34            | <b>29.67</b> | 27.39          | <b>22.51</b> | 27.78              | <b>28.23</b> | <b>26.47</b>   | <b>23.66</b> |
| Erase <i>Snoopy</i> and <i>Mickey</i> and <i>Spongebob</i> |               |        |               |              |                  |              |                |              |                    |              |                |              |
|                                                            | CS ↓          | FID ↑  | CS ↓          | FID ↑        | CS ↓             | FID ↑        | CS ↑           | FID ↓        | CS ↑               | FID ↓        | CS ↑           | FID ↓        |
| ConAbl                                                     | 24.92         | 112.66 | 26.46         | 63.95        | 25.12            | 102.68       | 27.36          | 46.47        | 27.72              | 48.24        | 26.37          | 26.71        |
| MACE                                                       | 19.86         | 175.43 | 19.35         | 140.13       | 20.12            | 143.17       | 19.76          | 110.12       | 21.03              | 128.56       | 23.39          | 66.39        |
| RECE                                                       | <b>18.17</b>  | 155.26 | <b>18.87</b>  | 149.77       | <b>16.23</b>     | 178.55       | 27.34          | 40.52        | 27.71              | 52.06        | 26.32          | 32.51        |
| UCE                                                        | 23.29         | 101.40 | 24.63         | 88.11        | 19.08            | 140.40       | 27.45          | 29.20        | 27.82              | 38.15        | 26.30          | 28.71        |
| Ours                                                       | 23.69         | 103.33 | 23.93         | 86.55        | 21.39            | 109.28       | 27.47          | <b>21.40</b> | 27.76              | <b>26.22</b> | <b>26.51</b>   | <b>24.99</b> |

Table 8. **Full quantitative comparison of the few-concept erasure in erasing instances from Table 1.** The erased target concept(s) are shaded in pink, the best results are highlighted in bold, and the grey columns are indirect indicators for measuring erasure efficacy on target concepts or prior preservation on non-target concepts.

space, we select the eigenvectors corresponding to the eigenvalues below  $10^{-1}$  on few-concept and implicit concept erasure and  $10^{-4}$  on multi-concept erasure following [14]. Moreover, since the retain set only includes ‘ ’ in implicit concept erasure, we add an identity matrix  $\mathbf{I}$  with weight  $\lambda = 0.5$  to the term  $(\mathbf{C}_2^T \mathbf{P} \mathbf{M} \mathbf{C}_2)^{-1}$  in Eq. 11 to ensure invertibility following [18].

## D. Additional Experiments

### D.1. Full Comparison on Few-Concept Erasure

We present full quantitative comparisons of few-concept erasure, including both CS and FID, in Table 8 and Table 9. Our results demonstrate that our method consistently achieves superior prior preservation, as indicated by higher CS and lower FID across the majority of non-target concepts.

### D.2. More Baselines

In this section, we compare against more methods because of the page limit in our main paper. Since our method focuses on improving prior preservation and multi-concept erasure performance, we mainly compare it with similar methods, other methods like ESD [17], FMN [66], and SLD [51] are omitted, as they fail to achieve satisfactory prior preservation proved by previous comparisons [35, 37, 62]. The remaining comparable method is SPM\*\* [37], which is proposed to improve prior preservation and can scale to multi-concept erasure tasks. Notable, SPM not only fine-tunes the model weights using LoRA [25] but also intervenes in the image generation process through *Facilitated Transport*. Specifically, this module dynamically adjusts the LoRA scale based on the similarity between the sampling prompt and the target concept. In other words, if the prompt contains the target concept or is highly relevant, this scale is set to a large value, whereas if there is little to no relevance, it is set close to 0, functioning similarly to a text filter. We argue that such a comparison with SPM is not fair since we only focus on modifying the model parameters, and therefore, we compare both the original SPM and SPM without *Facilitated Transport* (SPM w/o FT) for a fair comparison. In the latter version, the LoRA scale is set to 1 by default.

\*\*<https://github.com/Con6924/SPM>

|                       | <i>Van Gogh</i> |               | <i>Picasso</i> |               | <i>Monet</i> |               | <i>Paul Gauguin</i> |              | <i>Caravaggio</i> |              | MS-COCO      |              |
|-----------------------|-----------------|---------------|----------------|---------------|--------------|---------------|---------------------|--------------|-------------------|--------------|--------------|--------------|
|                       | CS              | FID           | CS             | FID           | CS           | FID           | CS                  | FID          | CS                | FID          | CS           | FID          |
| SD v1.4               | 28.75           | -             | 27.98          | -             | 28.91        | -             | 29.80               | -            | 26.27             | -            | 26.53        | -            |
| Erase <i>Van Gogh</i> |                 |               |                |               |              |               |                     |              |                   |              |              |              |
|                       | CS ↓            | FID ↑         | CS ↑           | FID ↓         | CS ↑         | FID ↓         | CS ↑                | FID ↓        | CS ↑              | FID ↓        | CS ↑         | FID ↓        |
| ConAbl                | 28.16           | 129.57        | 27.07          | 77.01         | 28.44        | 63.80         | 29.49               | 63.20        | 26.15             | 79.25        | 26.46        | <b>18.36</b> |
| MACE                  | 26.66           | 169.60        | 27.39          | 69.92         | 28.84        | 60.88         | 29.39               | 56.18        | 26.19             | 69.04        | 26.50        | 23.15        |
| RECE                  | 26.39           | <b>171.70</b> | 27.58          | 60.57         | 28.83        | 61.09         | 29.58               | 47.07        | 26.21             | 72.85        | 26.52        | 23.54        |
| UCE                   | 28.10           | 133.87        | 27.70          | 43.02         | 28.92        | 40.49         | 29.62               | 32.62        | 26.23             | 61.72        | 26.54        | 19.63        |
| Ours                  | <b>26.29</b>    | <b>131.02</b> | 27.96          | <b>35.86</b>  | 28.94        | <b>16.85</b>  | 29.71               | <b>24.94</b> | 26.24             | <b>39.75</b> | <b>26.55</b> | 20.36        |
| Erase <i>Picasso</i>  |                 |               |                |               |              |               |                     |              |                   |              |              |              |
|                       | CS ↑            | FID ↓         | CS ↓           | FID ↑         | CS ↑         | FID ↓         | CS ↑                | FID ↓        | CS ↑              | FID ↓        | CS ↑         | FID ↓        |
| ConAbl                | 28.66           | 60.44         | 26.97          | 131.45        | 28.72        | 36.23         | 29.68               | 65.23        | 26.20             | 79.12        | 26.43        | 20.02        |
| MACE                  | 28.68           | 59.58         | 26.48          | <b>137.09</b> | 28.73        | 37.02         | 29.71               | 46.35        | 26.23             | 66.20        | 26.47        | 22.86        |
| RECE                  | 28.71           | 51.09         | 26.66          | 126.40        | 28.87        | 25.39         | 29.69               | 46.08        | 26.22             | 75.61        | 26.48        | 23.03        |
| UCE                   | 28.72           | 37.58         | 26.99          | 102.21        | 28.92        | <b>16.72</b>  | 29.71               | 32.48        | 26.22             | 59.27        | 26.50        | 20.33        |
| Ours                  | 28.76           | <b>19.18</b>  | <b>26.22</b>   | 117.71        | 28.88        | 19.87         | 29.75               | <b>24.73</b> | 26.24             | <b>43.63</b> | <b>26.51</b> | <b>19.98</b> |
| Erase <i>Monet</i>    |                 |               |                |               |              |               |                     |              |                   |              |              |              |
|                       | CS ↑            | FID ↓         | CS ↑           | FID ↓         | CS ↓         | FID ↑         | CS ↑                | FID ↓        | CS ↑              | FID ↓        | CS ↑         | FID ↓        |
| ConAbl                | 28.58           | 68.77         | 27.43          | 64.25         | 27.05        | 96.67         | 29.09               | 57.33        | 26.09             | 71.88        | 26.45        | 21.03        |
| MACE                  | 28.56           | 61.50         | 27.74          | 48.41         | 25.98        | 116.34        | 29.39               | 49.66        | 25.98             | 65.87        | 26.47        | 22.76        |
| RECE                  | 28.63           | 56.26         | 27.88          | 45.97         | 25.87        | 121.28        | 29.43               | 46.38        | 26.20             | 64.19        | 26.49        | 24.94        |
| UCE                   | 28.65           | 42.25         | 27.91          | <b>38.73</b>  | 27.12        | 98.37         | 29.58               | 33.00        | 26.16             | 56.49        | <b>26.51</b> | 21.58        |
| Ours                  | 28.76           | <b>28.78</b>  | 27.93          | 41.21         | <b>25.06</b> | <b>134.11</b> | 29.66               | <b>27.85</b> | 26.22             | <b>55.20</b> | 26.48        | <b>20.87</b> |

Table 9. **Full quantitative comparison of the few-concept erasure in erasing styles from Table 2.** The erased target concept(s) are shaded in pink, the best results are highlighted in bold, and the grey columns are indirect indicators for measuring erasure efficacy on target concepts or prior preservation on non-target concepts.

The quantitative comparative results are shown in Table 10. It can be seen that our method consistently achieves the best prior preservation compared to both SPM and SPM w/o FT. Even equipped with *Facilitated Transport*, our method achieves the lowest non-target FID (e.g., on *Pikachu* and *Hello Kitty*). This superiority amplifies as the number of target concepts increases. For example, with the number of target concepts increasing from 1 to 3, our FID in *Pikachu* rises from 16.81 to 21.40 (4.59 ↑), while SPM increases from 19.82 to 37.51 (17.69 ↑), where a similar pattern is observed in *Hello Kitty* (Our 4.48 ↑ v.s. SPM’s 15.68 ↑). Once removing the *Facilitated Transport* module, SPM w/o FT shows poor erasure efficacy in multi-concept erasure (highlighted by red in Table 10 and illustrated in Fig. 8). This indicates that the success of SPM in multi-concept erasure relies on the *Facilitated Transport* module, which dynamically allocates the LoRA scales by calculating the similarity between the sampling prompt and each target concept. For example, when erasing *Snoopy + Mickey + SpongeBob*, if the sampling prompt is “a photo of *Snoopy*”, SPM will allocate a larger scale to *Snoopy*’s LoRA according to the text similarity. On the contrary, if the sampling prompt is “a photo of *Pikachu*” with the non-target concept, all three LoRA scales will be assigned lower values, thereby preserving the prior knowledge. We argue that this strategy of dynamically tuning the LoRA scales based on the sampling prompt similarity is vulnerable to attacks and easily bypassed, especially in white-box attack scenarios, where an attacker can reconstruct the erased concepts by simply modifying the code with extremely low attack costs, e.g., open-source T2I models like Stable Diffusion [1, 2].

### D.3. Ablation Studies

**Augmentation times.** We ablate the augmentation times  $N_A$  proposed in the Directed Prior Augmentation (DPA) module in Sec. 4.2, which controls the balance between rank saturation and prior coverage along with the Influence-based Prior Filtering (IPF) module. It can be observed from Fig. 9 (a) that: (1) As  $N_A$  increases, the non-target FID exhibits a trend of first decreasing and then increasing. This suggests that when  $N_A$  is small (i.e.,  $1 \rightarrow 10$ ), augmenting existing non-target concepts with semantically similar concepts facilitates a more comprehensive prior coverage, thereby improving prior preservation. However, when  $N_A$  exceeds a certain threshold (i.e.,  $10 \rightarrow 20$ ), further augmentation of non-target concepts leads to narrowing the null-space derivation due to rank saturation, ultimately degrading prior preservation. (2) Target CS

| Concept                                                    | <i>Snoopy</i> |        | <i>Mickey</i> |              | <i>Spongebob</i> |              | <i>Pikachu</i> |              | <i>Hello Kitty</i> |              |
|------------------------------------------------------------|---------------|--------|---------------|--------------|------------------|--------------|----------------|--------------|--------------------|--------------|
|                                                            | CS            | FID    | CS            | FID          | CS               | FID          | CS             | FID          | CS                 | FID          |
| SD v1.4                                                    | 28.51         | -      | 26.62         | -            | 27.30            | -            | 27.44          | -            | 27.77              | -            |
| Erase <i>Snoopy</i>                                        |               |        |               |              |                  |              |                |              |                    |              |
|                                                            | CS ↓          | FID ↑  | CS ↑          | FID ↓        | CS ↑             | FID ↓        | CS ↑           | FID ↓        | CS ↑               | FID ↓        |
| SPM                                                        | 23.72         | 116.26 | 26.62         | 31.21        | 27.21            | 31.96        | 27.41          | 19.82        | 27.80              | 30.95        |
| SPM w/o FT                                                 | 23.72         | 116.26 | 26.55         | 43.03        | 26.84            | 42.96        | 27.38          | 25.95        | 27.71              | 42.53        |
| Ours                                                       | <b>23.50</b>  | 108.51 | 26.67         | <b>23.41</b> | 27.31            | <b>24.64</b> | 27.42          | <b>16.81</b> | 27.82              | <b>21.74</b> |
| Erase <i>Snoopy</i> and <i>Mickey</i>                      |               |        |               |              |                  |              |                |              |                    |              |
|                                                            | CS ↓          | FID ↑  | CS ↓          | FID ↑        | CS ↑             | FID ↓        | CS ↑           | FID ↓        | CS ↑               | FID ↓        |
| SPM                                                        | <b>23.18</b>  | 122.17 | <b>22.71</b>  | 117.30       | 26.92            | 38.35        | 27.35          | 27.13        | 27.76              | 39.61        |
| SPM w/o FT                                                 | 26.66         | 83.11  | 25.64         | 75.46        | 26.73            | 42.30        | 27.50          | 28.19        | 27.75              | 41.19        |
| Ours                                                       | 23.58         | 103.62 | 23.62         | 83.70        | 27.24            | <b>29.67</b> | 27.39          | <b>22.51</b> | 27.78              | <b>28.23</b> |
| Erase <i>Snoopy</i> and <i>Mickey</i> and <i>Spongebob</i> |               |        |               |              |                  |              |                |              |                    |              |
|                                                            | CS ↓          | FID ↑  | CS ↓          | FID ↑        | CS ↓             | FID ↑        | CS ↑           | FID ↓        | CS ↑               | FID ↓        |
| SPM                                                        | <b>22.86</b>  | 125.66 | <b>22.08</b>  | 123.20       | <b>20.92</b>     | 153.36       | 27.50          | 37.51        | 27.63              | 46.63        |
| SPM w/o FT                                                 | 27.75         | 68.89  | 26.24         | 63.30        | 24.82            | 77.38        | 27.44          | 30.00        | 27.74              | 38.89        |
| Ours                                                       | 23.69         | 103.33 | 23.93         | 86.55        | 21.39            | 109.28       | 27.47          | <b>21.40</b> | 27.76              | <b>26.22</b> |

Table 10. **Quantitative comparison with SPM and SPM w/o FT (Facilitated Transport)**. The erased target concept(s) are shaded in pink, the best results are highlighted in bold, and the grey columns are indirect indicators for measuring erasure efficacy on target concepts or prior preservation on non-target concepts.

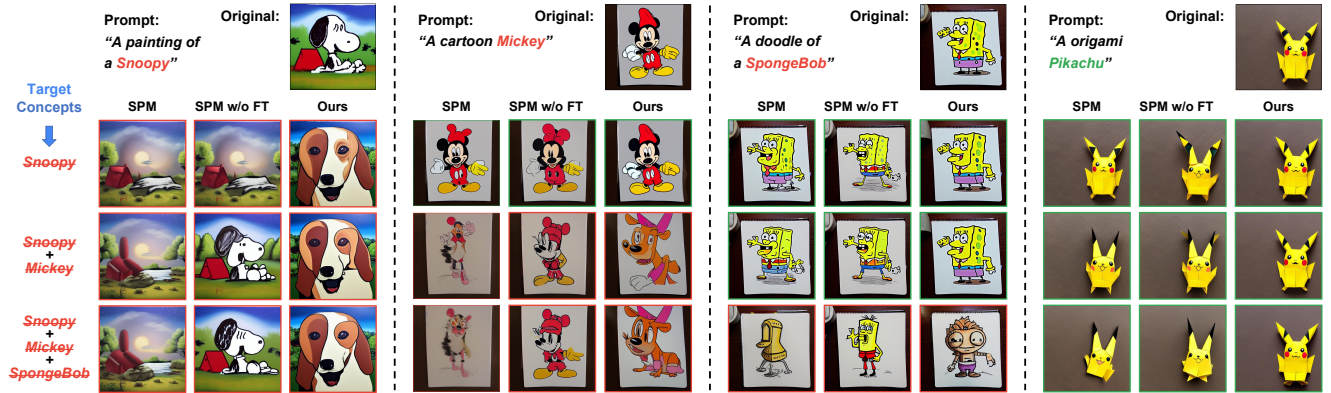


Figure 8. **Qualitative comparison with SPM and SPM w/o FT in erasing single and multiple instances**. The erased and preserved generations are highlighted with red and green boxes, respectively. Our method demonstrates superior prior preservation compared to both SPM and SPM w/o FT. Meanwhile, without the *Facilitated Transport* module, SPM w/o FT shows poor erasure efficacy in multi-concept erasure (e.g., the 1st case in *Snoopy*, 2nd case in erasing *Mickey*, and 3rd case in *SpongeBob*) with relatively high target CS in Table 10.

generally shows a declining trend, indicating that the proposed Prior Knowledge Refinement strategy not only improves prior preservation but also exerts a positive impact on erasure efficacy.

**Augmentation ranks.** Another hyperparameter to be ablated is the augmentation ranks  $r$ . From Eq. 6, we introduce the number of the smallest singular values, i.e., augmentation ranks  $r$  in deriving  $\mathbf{P}_{\min} = \mathbf{U}_{\min} \mathbf{U}_{\min}^T$  with  $\mathbf{U}_{\min} = \mathbf{U}_{\mathbf{W}}[:, -r :]$ . Mathematically,  $r$  represents the directions in which the DPA module can augment in the concept embedding space and constrains the rank of the augmented embeddings to a maximum of  $r$ . As shown in Fig. 9 (b), as  $r$  increases, the non-target FID exhibits an overall upward trend, indicating that introducing more ranks does not benefit prior preservation, as it narrows the null space. At the same time, as shown in Table 6, such augmentation by DPA also remains necessary, as it enables more comprehensive coverage of non-target knowledge with semantically similar concepts, leading to improved prior preservation.

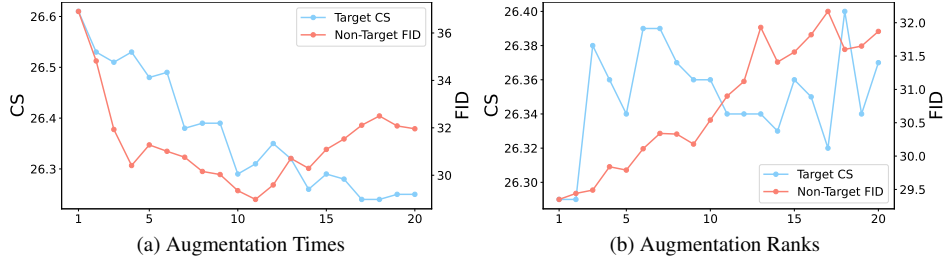


Figure 9. **Ablation study on two parameters, i.e., augmentation times  $N_A$  and augmentation ranks  $r$  of the DPA module.** We report the target CS of erasing *Van Gogh* and the non-target FID averaged over other four styles (i.e., *Picasso*, *Monet*, *Paul Gauguin*, *Caravaggio*).

| Ablation | Parameters |       | <i>Van Gogh</i> | <i>Picasso</i> | <i>Monet</i> | <i>Paul Gauguin</i> | <i>Caravaggio</i> | MS-COCO      |              |
|----------|------------|-------|-----------------|----------------|--------------|---------------------|-------------------|--------------|--------------|
|          | Key        | Value | CS ↓            | FID ↓          | FID ↓        | FID ↓               | FID ↓             | CS ↑         | FID ↓        |
| 1        | ✓          | ×     | 27.67           | 42.11          | 26.09        | 28.08               | 52.44             | <b>26.55</b> | <b>18.72</b> |
| 2        | ✓          | ✓     | <b>26.24</b>    | 48.41          | 28.65        | 33.79               | 57.23             | 26.53        | 23.20        |
| Ours     | ×          | ✓     | 26.29           | <b>35.86</b>   | <b>16.85</b> | <b>24.94</b>        | <b>39.75</b>      | <b>26.55</b> | 20.36        |

Table 11. **Ablation study on the edited parameters.** Our scheme on only editing the value matrices achieves a superior balance between erasure efficacy (e.g., target CS of 26.29) and prior preservation (e.g., the lowest FIDs across all non-target concepts).

| Metric             | <i>Van Gogh</i> | <i>Picasso</i> | <i>Monet</i> | <i>Paul Gauguin</i> | <i>Caravaggio</i> | MS-COCO      |              |
|--------------------|-----------------|----------------|--------------|---------------------|-------------------|--------------|--------------|
|                    | CS ↓            | FID ↓          | FID ↓        | FID ↓               | FID ↓             | CS ↑         | FID ↓        |
| Text Similarity    | 26.35           | 36.87          | 19.69        | 25.18               | 41.44             | 26.52        | 20.78        |
| Prior Shift (Ours) | <b>26.29</b>    | <b>35.86</b>   | <b>16.85</b> | <b>24.94</b>        | <b>39.75</b>      | <b>26.55</b> | <b>20.36</b> |

Table 12. **Ablation study on the importance metrics in IPF.**

**Edited parameters.** We compare the impact on editing different CA parameters in Table 11 and draw the following conclusions: (1) Only editing the key matrices cannot achieve effective erasure, with the target CS being 27.67 (v.s. the original CS of 28.75). This is because they mainly arrange the layout information of the generation and cannot effectively erase the semantics of the target concept. (2) Simultaneously editing both the key and value matrices can achieve effective erasure, but it will also excessively damage prior knowledge. (3) Only editing the value matrices achieves a superior balance between erasure efficacy and prior preservation. Compared to Ablation 2, the editing of key matrices leads to excessive erasure, which is unnecessary in concept erasure.

**Importance metrics in IPF.** In Sec. 4.1, we propose Importance-based Prior Filtering (IPF) in Eq. 5 and evaluate this importance with the metric prior shift =  $\|\Delta_{\text{erase}}c\|^2$ . Another intuitive and plausible metric is based on text similarity, e.g., the cosine similarity between each non-target embedding  $c_0$  and each target concept embedding  $c_1$ , i.e.,  $\cos(c_0, c_1)$ . Herein, we conduct an additional ablation study in terms of the metric selection in Table 12. It can be seen that text similarity can also serve as an effective metric for evaluating importance with improved non-target FID while the prior shift provides better prior preservation. This may be because text similarity is implicitly related to importance, while prior shift explicitly reflects the impact of erasure on different concepts from the model updates  $\Delta$ . Moreover, our method can be directly scaled up to multi-concept erasure scenarios, whereas text similarity calculates  $n$  similarities for  $n$  target concepts, requiring additional fusion or selection strategies, introducing accumulated errors during fusion or selection.

## E. Limitation

While SPEED demonstrates superior prior preservation, its erasure efficacy may not be as strong as some adversarial training/editing-based methods (e.g., RECE [19]), which explicitly optimize for robust concept removal. This trade-off arises from SPEED’s emphasis on maintaining non-target knowledge, potentially leading to residual traces of erased concepts in extreme cases. However, due to its efficiency and scalability in multi-concept erasure, an interesting direction for future work is to explore simultaneous erasure of adversarial examples. Given that null-space constraints inherently minimize the impact on prior knowledge, even with the addition of extra target concepts, SPEED is expected to achieve better prior preservation compared to existing methods while effectively handling adversarial concept erasure.